Journal of Energy Storage 82 (2024) 110592

Contents lists available at ScienceDirect

Journal of Energy Storage

journal homepage: www.elsevier.com/locate/est

Research papers

Self-healing distribution expansion planning considering distributed energy resources, electric vehicles parking lots and energy storage systems

Hossein Hosseini [a], Mehrdad Setayesh Nazar [a], Miadreza Shafie-khah [b], João P.S. Catalão [c,*]

[a] Faculty of Electrical Engineering, Shahid Beheshti University, Tehran, Iran
[b] University of Vaasa, 65200 Vaasa, Finland
[c] Research Center for Systems and Technologies (SYSTEC), Advanced Production and Intelligent Systems Associate Laboratory (ARISE), Faculty of Engineering, University of Porto, 4200-465 Porto, Portugal

ARTICLE INFO

Keywords:
Expansion planning
Self-healing
Consumer comfort
Smart appliances
Uncertainty modeling

ABSTRACT

This paper addresses an iterative optimization model for self-healing distribution expansion planning considering distributed energy resources, electric vehicles' parking lots, and energy storage systems. The main contribution of this model is that the smart devices of smart homes are modeled and the impacts of their commitments are explored in the expansion planning exercise. The proposed algorithm is another contribution of this paper that consists of tri-stage optimization processes. In the first stage, the optimal commitment of smart devices of smart homes is solved considering the worst-case external shock impacts on the consumers' comfort levels. Then, the optimal expansion planning of the distribution system is determined in the second stage problem. Finally, in the third stage, the optimal topology and dispatch of distributed energy resources are determined for the external shock conditions. The effectiveness of the proposed algorithm was assessed for the modified 123-bus system. Based on the simulation results, the aggregated costs of the 123-bus system were reduced by about 42.62 % using the proposed framework. Further, the expected energy not supplied costs of the system were reduced from 113 million monetary units to 0.284 million monetary units based on the fact that the model endeavored to minimize the interruption of critical loads.

1. Introduction

An electrical distribution system should be planned and operated in a way that it can tolerate stochastic shocks and recover to new steady-state conditions [1]. The most common practical planning paradigm of the electrical distribution systems is the N-1 criterion, which may not apply to natural catastrophic disasters [2]. Further, the unprecedented shock may reduce the residential consumers' comfort levels based on the duration and location of system outages.

A Self-Healing Electrical Distribution System (SHEDS) should consider the impacts of the system's shocks on the consumers' comfort levels in expansion planning practices. A SHEDS may utilize intermittent electricity generation facilities, electric vehicles' parking lots, energy storage systems, and Distributed Generation (DG) facilities [1].

Over the recent years, different aspects of SHEDS planning are presented and the impacts of external shocks on the distribution systems are explored. Gilasi et al. [3] introduced a model for allocating distributed energy resources. The model minimized the planning and operating costs. Further, the load shedding of the system in the external shock conditions was minimized. The non-dominated sorting genetic algorithm II using fuzzy decision-making was utilized to determine the Pareto solutions. Akbari et al. [4] explored a two-stage hybrid robust expansion-planning model that utilized a min-max-min optimization process considering the AC power flow. The column-and-constraint-generation process was used to find the best solution for the problem. Refs. [3, 4] did not consider the smart appliances' models, consumer comfort levels, and optimal microgrid formation of the distribution system. Zhou et al. [5] assessed a stochastic model for joint expansion planning of network and distributed energy resources considering intermittent electricity generation uncertainties. The system constraints considered radiality, reserve connection, and DG interconnections. The model minimized investment, operational, and environmental penalty costs. Firoozjaee et al. [6] proposed a hybrid expansion planning technique that determined the optimal penetration rate of microgrids. The model utilized a two-stage process. The first stage problem solved the generation and transmission expansion-planning problem. The second stage utilized the Monte-Carlo simulation process to determine the

* Corresponding author.
E-mail address: catalao@fe.up.pt (J.P.S. Catalão).

https://doi.org/10.1016/j.est.2024.110592
Received 28 May 2023; Received in revised form 7 January 2024; Accepted 13 January 2024
Available online 26 January 2024

Nomenclature

Abbreviations

ARIMA	Auto-Regressive Integrated Moving Average
DG	Distributed Generation
SHEDS	Self-Healing Electrical Distribution System
DRP	Demand Response Program
EENSC	Expected Energy Not Supplied Cost
MU	Monetary Unit
PHEV	Plug-in Hybrid Electric Vehicle
PV	Photovoltaic System
WT	Wind Turbine

Set and indices

K	Smart homes set
T	Daily simulation period set
N	Smart devices set
k	smart home index
t	Daily simulation period index
n	Smart device index
SD	The set of smart devices
j	External shock index
NES	External shock scenarios set
$NESEC$	The set of system switches
l	Switch index
$NCLS$	Comfort levels of consumers scenario set
m	Comfort level scenario index
NCS	Consumers set
m'	Consumer index
$NWMPS$	Wholesale market price scenarios set
r	Wholesale market price index
$NIEGS$	Intermittent energy generation scenarios set
r'	Intermittent energy generation scenario index

Scalars and parameters

a_k^{WD}, b_k^{WD}	The washing-drying machine parameters that consumer k determines based on his/her preference
a_k^{AC}, b_k^{AC}	The air conditioning system parameters that consumer k determines based on his/her preference
$Temp_k^{in}$, $Temp_k^{com}$	The inside and outside temperatures of the house
$Temp_k^{out}$	The outdoor temperature of the house
ξ	The heat transfer between the indoor and outdoor environments of the house
ϑ	The thermal efficiency of the air conditioner
a_k^{PHEV}, b_k^{PHEV}	The PHEV parameters that consumer k determines based on his/her preference
$p^{Light.comf}$	The desired brightness
a_k^{Ent}, b_k^{Ent}	The entertainment system parameters that consumer k determines based on his/her preference
$p^{Ent.comf}$	The desired entertainment
C_{INV}	Investment cost
$prob^{ES}$	Probability of external shock scenario
W	Weighting factor
$prob^{CL}$	Probability of consumers' comfort level
$prob^{WMP}$	Probability of wholesale market price
$prob^{IEG}$	Probability of intermittent energy generation facilities' electricity generation

Variables

E_k^{SD}	Energy consumption of smart device SD of smart home k
P_k^{SD}	Power consumption of smart device SD of smart home k
Φ_k^n	Smart home owner k welfare is defined as Φ_k^n that derives from using smart device n
Γ	Comfort level of consumer
$P_k^{SD\_CRI}$	Critical loads of kth consumer
$P_k^{SD\_DEF}$	Deferrable loads of kth consumer
$P_k^{SD\_INT}$	Interruptible loads of kth consumer
β^{INT}, β^{DEF}	The interruptible load fee and deferrable load fee.
I^{SHEDS}	Binary decision variable of facility investment
C_{OP}	Operational cost of distributed energy resource commitment
C_{IMP}	Cost of energy imported from wholesale market
ψ_{tk}^{CRI}	Binary decision variable of critical load commitment
ψ_{tk}^{DEF}	Binary decision variable of deferrable load commitment
ψ_{tk}^{INT}	Binary decision variable of interruptible load commitment
C_k^{CRI}	Cost of critical load that is not committed
C_k^{DEF}	Cost of deferrable load that is not committed
C_k^{INT}	Cost of interruptible load that is not committed
X	Binary decision variable of switch status
$p_k^{WD}(t)$	power consumption of washing-drying machine
$p_k^{AC}(t)$	power consumption of the air conditioning system
$p_k^{PHEV}(t)$	power consumption of plug-in hybrid electric vehicle
$p_k^{Light}(t)$	power consumption of the lighting system
$p_k^{Ent}(t)$	power consumption of entertainment system

expected demand not served values and calculate the resilience index. Masoumi-Amiri et al. [7] introduced a bi-level optimization framework for expansion planning that maximized the microgrid owner profit and minimized the investment and operating costs of the planning problem. The microgrid and distribution system optimization models were solved in the upper-level and lower-level problems, respectively. Refs. [5–7] did not model consumer comfort levels and smart appliances' commitment. Further, the optimal demand response pricing process was not considered in these papers. Nasri et al. [8] proposed a six-step framework for expansion planning of the distribution system. The basic network topology formation and hurricane occurrence simulation were carried out in the first and second steps, respectively. The reinforcement process of the network in a preventive way and the operating optimization processes were performed in the third and fourth steps, respectively. Finally, the resiliency assessment and overall optimization of the formulated problems were considered in the fifth and sixth steps, respectively. Shahbazi et al. [9] introduced a resilient architecture strategy for a distribution system that utilized backup DGs and network hardening. The investment, operating, and resiliency objective functions were considered in the optimization process. The uncertainties of energy price, loads, and outages were modeled using stochastic models. Refs. [8, 9] did not explore the optimal microgrid formation of the distribution system in external shock conditions, smart appliance models, and consumer comfort levels.

Mousavizadeh et al. [10] assessed the resiliency level of a distribution system considering microgrid formations. The worst-case external shocks were modeled and multiple switching scenarios and uncertainties of loads were considered. Wu et al. [11] proposed a stochastic optimization model that determined the optimal allocation and sizing of energy resources considering the system's shocks. The mixed-integer linear programming was utilized to solve the problem and the survivability level of the system was evaluated. Gilani et al. [12] introduced a linear model to restore critical loads of the system and a multi-micro grid formation process was utilized to reduce the impacts of the worst-case external shock. The uncertainties of intermittent electricity generations and loads were modeled. Bessani et al. [13] explored a time-to-

Table 1
Comparison of the proposed method with other papers.

Ref.		3	4	5	6	7	8	9	10	11	12	13	14	15	16	17	18	Proposed Approach
Consumer comfort level		×	×	×	×	×	×	×	×	×	×	×	×	×	×	×	×	✓
Microgrid formation		×	×	×	×	×	×	×	✓	×	✓	×	×	×	✓	✓	×	✓
Csmart appliances commitment		×	×	×	×	×	×	×	×	×	×	×	×	×	×	×	×	✓
Method	MILP	×	✓	×	×	×	×	×	×	✓	✓	×	×	×	✓	✓	×	×
	MINLP	×	×	×	×	×	×	✓	×	×	×	×	×	×	×	×	×	×
	Heuristic	✓	×	✓	✓	✓	✓	×	✓	×	×	✓	✓	✓	×	×	✓	✓
Model	Deterministic	✓	×	✓	✓	✓	✓	×	✓	×	✓	✓	×	×	✓	✓	×	×
	Stochastic	×	✓	×	×	×	×	✓	×	✓	×	×	✓	✓	×	×	✓	✓
Pricing process for DRP		×	×	×	×	×	×	×	×	×	×	×	×	×	×	×	×	✓
Objective Function	Revenue of consumers	×	×	×	×	×	×	×	×	×	×	×	×	×	×	×	×	✓
	Gen. Cost	✓	✓	✓	✓	✓	✓	✓	×	×	✓	✓	✓	✓	✓	✓	✓	✓
	Storage Cost	×	×	✓	×	×	×	×	×	×	×	×	×	×	×	×	✓	✓
	Secu. Costs	✓	✓	✓	✓	✓	✓	✓	✓	×	×	✓	✓	✓	✓	✓	✓	✓
	PHEV cost	×	×	×	×	×	×	×	×	×	×	×	×	×	×	×	✓	✓
	DRP costs	×	×	×	×	×	×	×	×	×	×	×	×	×	×	×	✓	✓
	WT	✓	×	×	×	×	×	×	×	✓	✓	×	×	×	×	×	✓	✓
	PV	✓	×	×	×	×	×	×	×	✓	✓	×	×	×	×	×	✓	✓
Uncertainty Model	PHEV	×	×	×	×	×	×	×	×	×	×	×	×	×	×	×	✓	✓
	External Shock	×	×	×	×	×	×	✓	×	×	×	×	✓	✓	×	×	✓	✓
	Loads	×	✓	×	×	×	×	✓	✓	×	✓	×	×	×	×	×	✓	✓
	Intermittent electricity generation	×	✓	×	×	×	×	✓	×	✓	✓	×	×	×	×	×	✓	✓

event model that assessed the structural resilience of the system. The performance and structural indices were utilized to assess the post-contingency conditions and the resiliency levels of the system were analyzed in shock conditions. Refs. [10–13] did not assess the impacts of smart appliances' commitment and consumer comfort levels on the expansion-planning problem. Further, the demand response pricing process was not modeled in these papers. Wei Yuan et al. [14] utilized the N—K contingency method to assess the resiliency of the distribution system. The column constraint generation decomposition was utilized for the proposed two-stage robust optimization algorithm. The network hardening and DGs' allocations were modeled in the problem. Bahramabadi et al. [15] utilized a model to allocate the switching device allocation and enhance the resiliency level of the system. The extreme weather condition was modeled in the first stage. Further, the resiliency index was determined in the second stage. Refs. [14, 15] did not model the smart appliances models and consumer comfort levels. Mishra et al. [16] proposed an algorithm for optimal resilient expansion planning considering the coordinated operational scheduling of microgrids. The worst-case contingency was considered an external shock and a mixed-integer linear programming algorithm was utilized to solve the problem. Lin et al. [17] assessed a defender-attacker-defender model to enhance the resiliency level of the system. The model consists of three stages and the hardening process was carried out in the first stage. The worst-case external shock and resilient operating conditions were analyzed in the second and third stages, respectively. Zakernezhad et al. [18] presented a multi-stage expansion planning optimization algorithm that considered the capacity withholding process of non-utility electricity generation facilities. The model assessed the bidding strategies of non-utility generations and calculated the withholding indices to explore the value of withholdings. Refs. [16–18] did not model smart appliances and consumer comfort levels. The smart appliances' commitment can change the available energy resources of the distribution systems in normal and external shock conditions. An integrated model that considers the consumer comfort levels and smart appliances' commitment in the expansion planning exercise is less frequent in the literature. Table 1 shows the comparison of the proposed model with the other papers.

The main contributions of this paper are:

- The optimization model determines the optimal topology of the distribution system and smart appliances' commitment in the worst-case external shock;
- The proposed algorithm models the consumer comfort levels and smart appliances commitment in the expansion planning of the distribution system;
- The model presents a pricing algorithm for determining the optimal values of interruptible and deferrable electricity consumption of smart home appliances.

2. Problem modeling and formulation

A self-healing electrical distribution system can transact energy with smart homes in normal and shock conditions. It is assumed that the SHEDS has multiple distributed energy resources and PHEV parking lots and transacts electricity with the wholesale electricity market. Further, it is assumed that there is not any local electricity market in the SHEDS, and all of the distributed energy resources and PHEV parking lots are centrally controlled by the SHEDS operator.

At the first-stage optimization process, the optimal scheduling of smart home appliances is carried out. Then, in the second stage problem, the optimal expansion planning of the self-healing distribution system is performed. Finally, in the third-stage problem, the optimal scheduling of the distribution system in external shock conditions is determined. The following subsections present the detailed modeling and formulation of the proposed method.

2.1. First-stage problem formulation

The optimization process consists of 24 snapshots and t represents the daily simulation period$t \in T = \{1, 2, \ldots, 24\}$ [19]. It is assumed that the SHEDS supplies K smart homes and $k \in K$ presents each smart home. Further, each smart home has a set of smart devices (N), and $n \in N$ presents each smart device. Thus, the energy and power consumption of smart home k can be presented as E_k^{SD} and P_k^{SD}, respectively.

It is assumed that each smart home has the following smart devices: 1) a washing-drying machine, 2) an air conditioning system, 3) a plug-in hybrid electric vehicle (PHEV), 4) a lighting system, and 5) an entertainment system [19]. Thus, the following set can be defined: SD = {washing-drying machine, air conditioning system, PHEV, lighting system, entertainment system}.

The smart homeowner k welfare is defined as Φ_k^n that derived from using smart device n. Further, Φ_k^n can be represented as the electricity consumption cost of device n. Thus, the comfort level of the consumer is defined as Γ which equals the net welfare of the consumer. The net welfare of the consumer equals his/her comfort level minus the cost of his/her electricity consumption. Thus, the higher value of Γ corresponds to the higher value of the comfort level of the consumer. The welfare that the consumer derives from using the smart device k can be categorized into the following equations:

A. Washing-drying machine:

The welfare of the consumer derived from using the washing-drying machine can be presented as Eq. (1):

$$\Phi_k^{WD} = a_k^{WD} E_k^{WD} + b_k^{WD} \tag{1}$$

where, a_k^{WD} and b_k^{WD} are parameters that consumer k determines based on his/her preference. T_k^{WD} presents the set of times that the washing-drying machine is utilized. The following constraints are considered for the washing-drying machine.

- Eq. (2) presents the maximum value of power consumption for the washing-drying machine.

$$0 \le p_k^{WD}(t) \le p_k^{WD\ Max}, \forall t \in T_k^{WD} \tag{2}$$

- Eq. (3) considers the aggregated power consumption of washing-drying machine.

$$E_k^{WD\ Min} \le \sum_{T_k^{WD}} p_k^{WD}(t) \le E_k^{WD\ Max}, \forall t \in T_k^{WD} \tag{3}$$

where, $p_k^{WD\ Max}$, $E_k^{WD\ Min}$, and $E_k^{WD\ Max}$ are maximum power consumption, minimum energy consumption, and maximum energy consumption of the washing-drying machine, respectively.

B. Air conditioning system:

The welfare of the consumer derived from using the air conditioning system can be formulated as Eq. (4):

$$\Phi_k^{AC} = a_k^{AC} - b_k^{AC}\left(Temp_k^{in} - Temp_k^{com}\right)^2 \tag{4}$$

where, a_k^{AC} and b_k^{AC} are selected by consumer k. $Temp_k^{in}$ and $Temp_k^{com}$ are the inside temperature of the house and the comfort temperature of the consumer. T_k^{AC} presents the set of times that the air conditioning system is utilized. Further, the following equations are constraints for the air conditioning system.

- Eq. (5) presents the maximum value of power consumption for the air conditioning system.

$$0 \le p_k^{AC}(t) \le p_k^{AC\ Max}, \forall t \in T_k^{AC} \tag{5}$$

- The minimum and maximum values of inside temperature should be considered as constraints of the air conditioning system, which is presented in Eq. (6).

$$Temp_k^{com\ Min} \le Temp_k^{in}(t) \le Temp_k^{com\ Max} \tag{6}$$

where, $Temp_k^{com\ Min}$ and $Temp_k^{com\ Max}$ are the minimum and maximum values of comfort temperature of the consumer's house.

- The air-conditioning system controls the inside temperature of the consumer's house based on Eq. (7), which $Temp_k^{out}(t)$ is the outside temperatures of the consumer's house:

$$Temp_k^{in}(t) = Temp_k^{in}(t-1) + \xi \cdot \left(Temp_k^{out}(t) - Temp_k^{in}(t-1)\right) + \vartheta \cdot p_k^{AC}(t) \tag{7}$$

where, ξ is the heat transfer between the indoor and outdoor environments of the house, and θ is the thermal efficiency of the air conditioner [19].

C. Plug-in hybrid electric vehicle:

The welfare of the consumer derives from using the plug-in hybrid electric vehicle is formulated as Eq. (8):

$$\Phi_k^{PHEV} = a_k^{PHEV} \cdot E_k^{PHEV} + b_k^{PHEV} \tag{8}$$

where, a_k^{PHEV} and b_k^{PHEV} are adjusted by the consumer k based on his/her preferences. The following constraints are considered for the plug-in hybrid electric vehicle.

- Eq. (9) presents the maximum value of the charging power of the plug-in hybrid electric vehicle.

$$0 \le p_k^{PHEV}(t) \le p_k^{PHEV\ Max}, \forall t \in T_k^{PHEV} \tag{9}$$

- Eq. (10) considers the aggregated energy charging and discharging of plug-in hybrid electric vehicles.

$$E_k^{PHEV\ Min} \le \sum_{T_k^{PHEV}} Ef_k^{PHEV} \cdot p_k^{PHEV}(t) \le E_k^{PHEV\ Max}, \forall t \in T_k^{PHEV} \tag{10}$$

where, p_k^{PHEV}, $E_k^{PHEV\ Min}$, $E_k^{PHEV\ Max}$, and Ef_k^{PHEV} are maximum power consumption, minimum energy consumption, maximum energy consumption, and energy efficiency of the battery system of the plug-in hybrid electric vehicle, respectively. Further, T_k^{PHEV} presents the set of times that the plug-in hybrid electric vehicle is utilized.

D. Lighting system:

The welfare of the consumer derives from using the lighting system is formulated as Eq. (11):

$$\Phi_k^{Light} = a_k^{Light} - b_k^{Light}\left(p_k^{Light} - p_k^{Light.comf}\right)^2 \tag{11}$$

where, a_k^{Light} and b_k^{Light} are adjusted by the consumer k. $p^{Light.comf}$ is the desired brightness. The following equations are constraints for the lighting system.

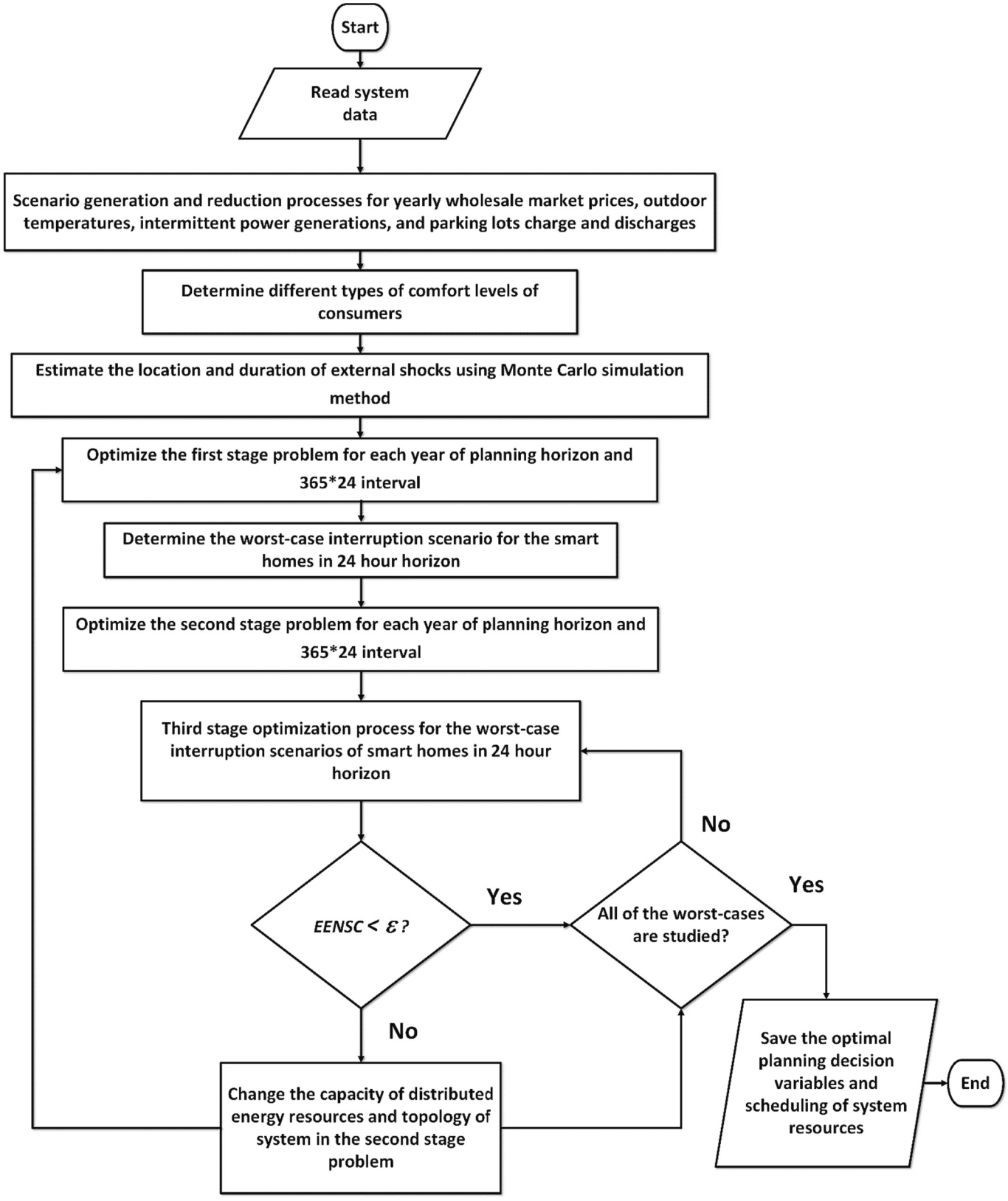

Fig. 1. The flowchart of the suggested procedure.

- Eq. (12) presents the maximum value of power consumption for the lighting system.

$$0 \le p_k^{Light}(t) \le p_k^{Light\ Max}, \forall t \in T_k^{Light} \tag{12}$$

where, p_k^{Light} and T_k^{Light} are the maximum power consumption of the lighting system and the set of times that the system is utilized, respectively.

E. Entertainment system:

The welfare of the consumer derived from using the entertainment system can be formulated as Eq. (13):

$$\Phi_k^{Ent} = a_k^{Ent} - b_k^{Ent}\left(p_k^{Ent} - p_k^{Ent.comf}\right)^2 \tag{13}$$

where, a_k^{Ent} and b_k^{Ent} are adjusted by the consumer k. $p^{Ent.comf}$ is the desired entertainment. The following equations are constraints for the entertainment system.

- Eq. (14) presents the maximum value of power consumption for the entertainment system.

$$0 \le p_k^{Ent}(t) \le p_k^{Ent\ Max}, \forall t \in T_k^{Ent} \tag{14}$$

where, p_k^{Ent} and T_k^{Ent} are the maximum power consumption of the entertainment system and the set of times that the system is utilized, respectively. More detailed models of smart appliances are presented in [19] and are not presented for the sake of space. The consumer k endeavors to maximize his/her net welfare. It is assumed that the home energy management system determines the initial values of a and b parameters of smart devices and communicates with the SHEDS based on the smart grid infrastructure. Thus, the objective function of the first stage optimization problem can be defined as (15):

$$Max\ \Gamma_k = Max \sum_{t\in T}\left(\sum_{n\in N}\left(\Phi_{ktn}^{SD} - C_{ktn}^{SD}\right)\right) \quad \forall \in \{WD, AC, PHEV, Light, Ent\}$$

$$S.t: H_1(x,y,z) = 0, \quad G_1(x,y,z) \ge 0 \tag{15}$$

where, C_{ktn}^{SD} is the kth consumer energy consumption cost at the time t for using device n of set SD = {washing-drying machine, air conditioning system, PHEV, lighting system, entertainment system}. Eq. (15) is constrained by Eqs. (2), (3), (5), (6), (7), (9), (10), (12), (14) [19]. The compact form of the first stage problem is presented as $H_1(x,y,z) = 0$, $G_1(x,y,z) \ge 0$ that x, y, and z are control, state, and topology variables, respectively.

Based on Eq. (15), the home energy management system of consumer k can prioritize its smart device power and energy consumption in the following groups. It is assumed that the SHEDS communicates with the energy management system of the smart home and it can pay capacity and option fees to consumers to encourage them to participate in the Demand Response Programs (DRPs).

- The interruptible loads ($P_k^{SD\_INT}$) that consist of the entertainment system and PHEV when its state of charge is higher than a predetermined level.

Based on the above categorization, any change in the volume and time of consumers' energy consumption can reduce their comfort levels. Thus, the SHEDS should pay consumers the interruptible load fee and deferrable load fee to compensate for the reduction of comfort levels and encourage the consumer to participate in the DRPs. Thus, Eq. (15) can be rewritten as (16) considering the consumer load priorities:

$$Max\ \Gamma_k = Max \sum_{t\in T}\left(\sum_{n\in N}\left(\Phi_{ktn}^{SD} + \beta_{ktn}^{\ DEF}\cdot P_{ktn}^{SD\_DEF} + \beta_{ktn}^{\ INT}\cdot P_{ktn}^{SD\_INT} - C_{ktn}^{SD}\right)\right)$$

$$\forall \in \{WD, AC, PHEV, Light, Ent\}$$

$$S.t: H_1(x,y,z) = 0, \quad G_1(x,y,z) \ge 0 \tag{16}$$

where, β^{INT} and β^{DEF} are the interruptible load fee and deferrable load fee, respectively.

Based on the proposed optimization model, the values of β^{INT} and β^{DEF} are decision variables of SHEDS, and higher values of these variables can compensate for the reduction in consumers' comfort levels.

The initial value of β^{INT} can be calculated from the following procedure: At first, the value of Eq. (16) is calculated for $\beta^{DEF} = 0$ and when the consumers are reducing the volume of their energy consumption using only the interruptible load demand response program. The initial value of β^{INT} should be selected in the manner that the value of Eq. (16) is equal to Eq. (15) based on the fact that the interruptible load fee is paid to compensate for the reduction in consumers' comfort levels for their contribution in interruptible load DRP.

Further, in the same procedure, the initial value of β^{DEF} is calculated based on the following process: the value of Eq. (16) is calculated for $\beta^{INT} = 0$ and when the consumers are reducing the volume of their energy consumption using only the deferrable load demand response program. The initial value of β^{DEF} should be calculated in the way that the value of Eq. (16) is equal to Eq. (15) because the deferrable load fee is paid to compensate for the reduction in consumers' comfort levels for their contribution to deferrable load DRP. Different comfort levels of consumers should be considered to generate different values of β^{INT} and β^{DEF} that are considered in the second and third stage optimization processes.

$$Max\ \mathfrak{M}_2 = \sum_{i=1}^{NYear}\sum_{r=1}^{NWMPS} prob_r^{WMP}\cdot\sum_{r'=1}^{NIEGS} prob_{r'}^{IEG}\cdot\left[\sum_{t=1}^{T}\left(-C_{INV\ i}\cdot I_i^{SHEDS} - C_{OP\ it} - C_{IMP\ it}\right) + \sum_{m'=1}^{NCS}\sum_{m=1}^{NCLS} prob_m^{CL}\cdot\sum_{t=1}^{T}\sum_{k=1}^{K}\Gamma_{m'itk} - \mathfrak{M}_3\right] \tag{17}$$

$$S.t: H_2(x,y,z) = 0, \quad G_2(x,y,z) \ge 0$$

- The critical loads ($P_k^{SD\_CRI}$) that consist of the lighting system (at night), PHEV when its state of charge is lower than a predetermined level, and air conditioning system,
- The deferrable loads ($P_k^{SD\_DEF}$) that consist of washing-drying machines,

2.2. Second-stage problem formulation

The expansion planning should maximize the social welfare of overall system participants, which consists of minimizing SHEDS investment, operating, and energy purchasing costs, and maximizing consumers' welfare in normal and shock conditions for the planning horizon.

Thus, the objective function of the expansion-planning problem can be presented as (17):

The objective function consists of 1) the investment costs of SHEDS ($C_{INV\,i} \cdot I_i^{SHEDS}$), 2) the operating costs of SHEDS in the normal operating condition of the system (C_{OP}), 3) the cost of imported active and reactive powers (C_{IMP}), and 4) the net welfare of consumers ($\sum_{k=1}^{K} \Gamma_{itk}$). Further, $prob^{CL}$, $prob^{WMP}$, and $prob^{IEG}$ are the probability of comfort level of consumers, probability of wholesale market price, and probability of intermittent energy generation facilities, respectively. $prob^{CL}$ is considered to encounter the probability of different types of consumers' comfort levels in the expansion planning process. I_{it}^{SHEDS} is the binary decision variable of distribution facility investment for the i^{th} year of planning horizon and t^{th} hour and it is assumed that the installation of facilities are performed in the beginning of each year of the planning years. Γ_{itk} are the comfort levels of consumers that are determined in the first stage problem and $\mathfrak{M}_3$ is the objective function of the third-stage optimization process. C_{INV} is the investment costs of distributed energy resources, switches, energy storages, and parking lots [2]. C_{OP} is the normal operating costs of distributed energy resources, switches, energy storages, and parking lots [2]. C_{IMP} is the cost of energy that is imported from the wholesale market.

The second-stage problem constraints are decomposed into 1) AC load-flow, 2) device-loading constraints, 3) supply-demand balancing constraints, 4) static-security constraints, and 5) radiality constraints that are available in [2]. The compact form of the second stage problem is presented as $H_2(x,y,z) = 0, \quad G_2(x,y,z) \geq 0$ that x, y, and z are control, state, and topology variables, respectively.

Based on the proposed formulation for Eqs. (16) and (17), it leads to the conclusion that the values of Γ (consumers' comfort levels) are initially determined in the first stage optimization problem. However, the consumers' comfort levels are determined in the second stage optimization process considering the expansion planning alternatives and uncertainties of the wholesale market, intermittent electricity generation facilities, and external shock conditions. Further, the optimal values of Eq. (17) are determined when the precise value of the objective function of the third stage optimization is calculated in the higher number of iterations.

2.3. Third-stage problem formulation

The third-stage optimization process considers the optimal commitment of consumers' loads and attempts to determine the optimal switching process of system switches in external shock conditions. This process endeavors to minimize the expected costs of critical loads, deferrable loads, and interruptible loads that are not committed considering the external shock conditions using the switching process of the system's switches. The objective function of the third stage problem can be described as (18):

$$
\begin{aligned}
&Min\ \mathfrak{M}_3 = \sum_{j=1}^{NES} prob_j^{ES} \cdot \left(\sum_{t=1}^{T} W_1 \cdot EENSC + W_2 \cdot \sum_{l=1}^{NESEC} X_{tl} \right) \\
&EENSC = \sum_{m'=1}^{NCS} \sum_{m=1}^{NCLS} prob_m^{CL} \cdot \sum_{k=1}^{K} \left(C_{m'tk}^{CRI} \cdot P_{m'tk}^{SD\_CRI} \left(1 - \psi_{m'tk}^{CRI}\right) + C_{m'tk}^{DEF} \cdot P_{m'tk}^{SD\_DEF} \cdot \psi_{m'tk}^{DEF} + C_{m'tk}^{INT} \cdot P_{m'tk}^{SD\_INT} \cdot \psi_{m'tk}^{INT} \right) \\
&S.t : H_3(x,y,z) = 0, \quad G_3(x,y,z) \geq 0
\end{aligned}
\tag{18}
$$

where, C^{CRI}, C^{DEF}, and C^{INT} are the costs of critical loads, deferrable loads, and interruptible loads that are not committed, respectively. $prob^{ES}$ is the probability of external shock occurrence. Further, ψ^{CRI}, ψ^{DEF}, and ψ^{INT} are the commitment decision variables of critical loads, deferrable loads, and interruptible loads, respectively. X is the binary decision variable that determines the status of the switch and the zero value X means the switch is open. W is the weighting factor. $EENSC$ is the expected energy not supplied costs that its formulation is presented in Eq. (18).

The third-stage problem constraints consist of 1) AC load-flow, 2) SHEDS device-loading constraints, 3) limits of electricity generation and ramp rates of power generation facilities, 4) supply-demand balancing constraints, 5) the constraints of energy storage facilities that are categorized into the state of charge constraints and the maximum charge limits, 6) static-security constraints, and 7) radiality constraints. The compact form of the third stage problem is presented as $H_3(x,y,z) = 0$, $G_3(x,y,z) \geq 0$ that x, y, and z are control, state, and topology variables, respectively.

By comparing Eq. (15) and Eq. (18) it can be concluded that the consumers' comfort levels in normal and external shock conditions are not equal based on the fact that Eq. (18) endeavors to optimally find the values of the critical loads, deferrable loads, and interruptible loads based on their contingent condition of SHEDS and available electricity generation of distributed energy generation facilities.

3. Solution algorithm

The proposed model is an iterative mixed-integer non-linear programming. The linearization technique is adopted to linearize the first and second problems. The CPLEX solver of GAMS is utilized to solve the first and second problems. The KNITRO solver of GAMS is utilized to solve the third problem. The following procedures and assumptions are considered:

- Different types of uncertainties are considered in the proposed model that consist of the following parameters: Wholesale market price scenarios that are considered in the second stage of the optimization process. Any change in wholesale electricity market prices can change the optimal volume of electricity transactions of distribution with the wholesale market and change the values of capacity, location, and the volume of distributed energy resources.
- Three comfort levels of consumers are considered to generate different values of β^{INT} and β^{DEF} for the second and third stage optimization processes. The value of $prob^{CL}$ is considered 0.33 for each consumer's comfort level.
- Different scenarios of intermittent electricity generation facilities are considered [2].
- Numerous scenarios for the state of charge of plug-in hybrid electric vehicles are generated. The state of charge constraints and the minimum energy level of plug-in hybrid electric vehicles are considered in the optimization process [2].

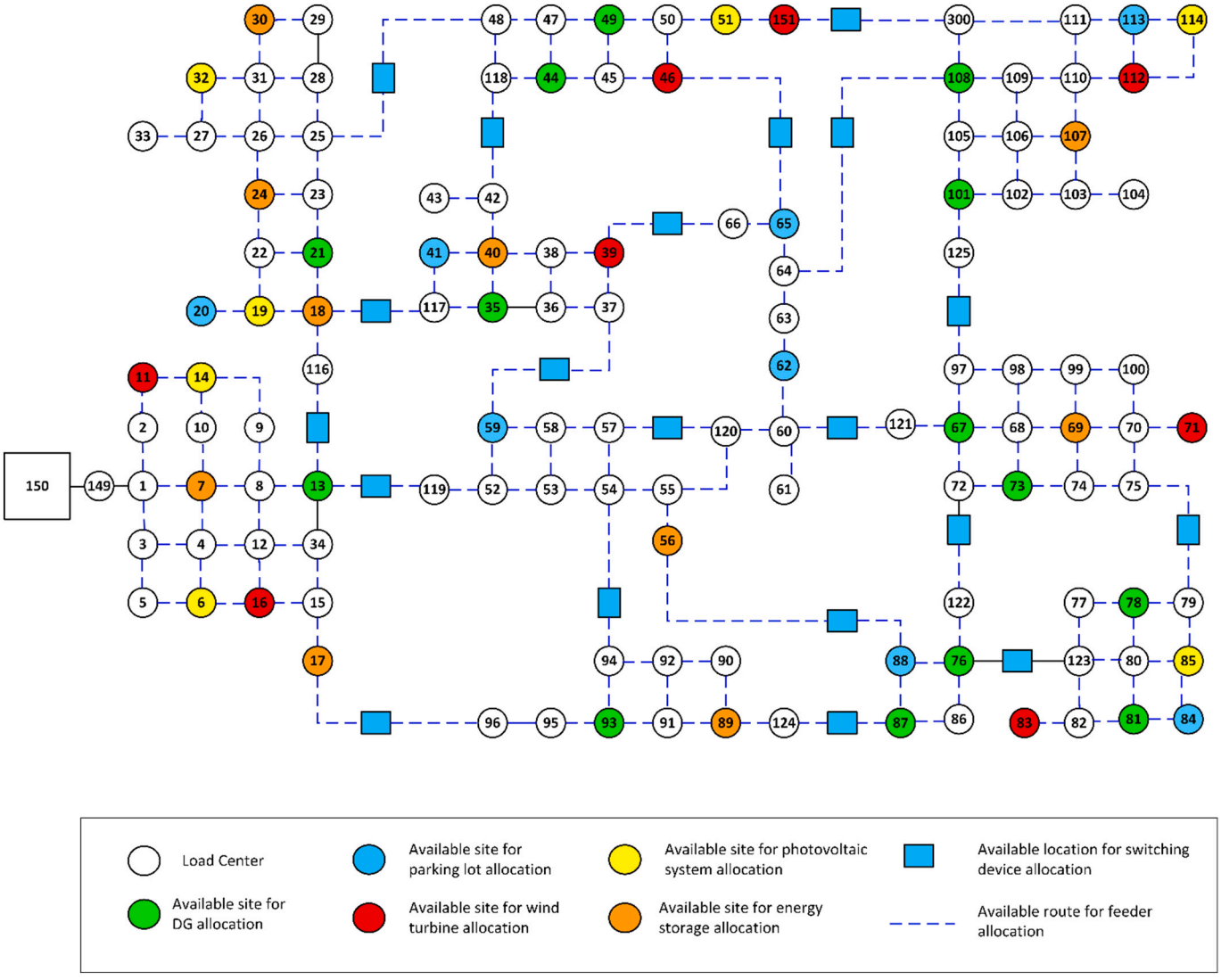

Fig. 2. The modified 123-bus test system.

- Multiple scenarios are considered for the hourly outdoor temperatures.
- The Auto-Regressive Integrated Moving Average (ARIMA) algorithm is utilized to model the wholesale market price, plug-in hybrid electric vehicles' electricity transactions, hourly outdoor temperature, and intermittent electricity generation [2].
- The magnitude and location of external shocks are determined by the Monte-Carlo simulation process [2]. The values of $prob^{ES}$ are calculated based on the Monte-Carlo simulation process.
- The AC load flow constraints were linearized using the proposed model of Ref. [20]. The error of the linearization method is formulated as Eq. (19):

$$\varepsilon^{'} = \left[1/cos\left(\pi/2^{\varpi+1}\right)\right] - 1 \tag{19}$$

where, ϖ is a parameter that determines the number of additional variables and constraints that are added to the constraint to linearize the AC load flow equations [20]. It was assumed: $\varpi = 15$. Thus, the error of the linearization method was $\varpi = 1.148973\ E - 9$. The details of the linearizing process are available in Ref. [20] and are not presented for the sake of space.

Fig. 1 presents the flowchart of the proposed optimization process. As shown in Fig. 1, at first, the scenario generation and reduction processes are performed for yearly wholesale market prices, outdoor temperatures, intermittent power generations, and parking lots' charges and discharges. Then, different types of comfort levels of consumers should be determined. The location and magnitude of external shocks are determined by the Monte-Carlo simulation process. Then, the worst-case contingency selection process is utilized to model the duration of external shocks.

Table 2
The scenario generation and reduction scenarios.

System parameter	Value
Number of solar irradiation scenarios	50
Number of wind turbine power generation scenarios	50
Number of hourly temperature scenarios	50
Number of wholesale market price scenarios	25
Number of plug-in hybrid electric vehicles scenarios	25
Number of solar irradiation-reduced scenarios	5
Number of wind turbine power generation reduced scenarios	5
Number of hourly temperature-reduced scenarios	5
Number of wholesale market price reduced scenarios	5
Number of plug-in hybrid electric vehicles reduced scenarios	5

At the first stage of the optimization process, the data of different types of smart homes and their smart appliances are uploaded. The first stage optimization process is performed and the values of interruptible,

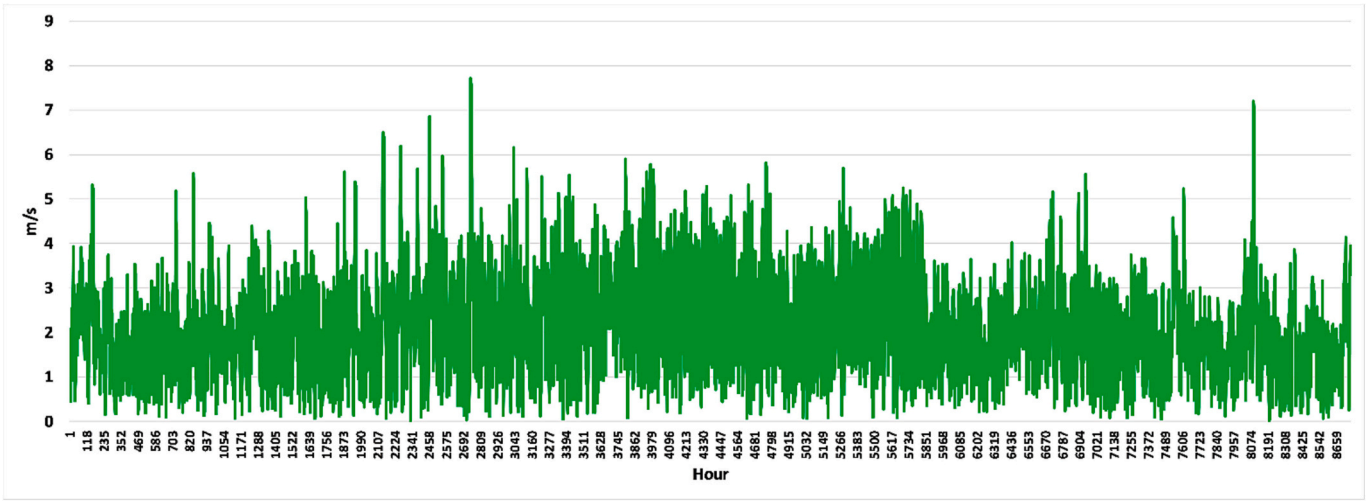

Fig. 3. The hourly wind speed of the planning site for the horizon year and one of the reduced scenarios.

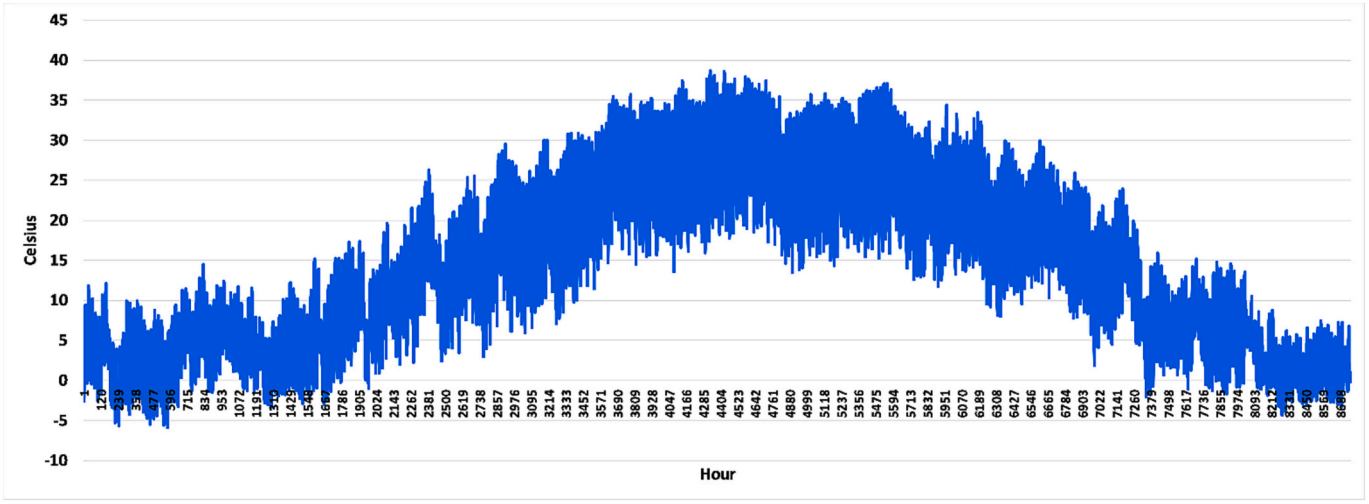

Fig. 4. The estimated hourly temperature of the planning site for the horizon year and one of the reduced scenarios.

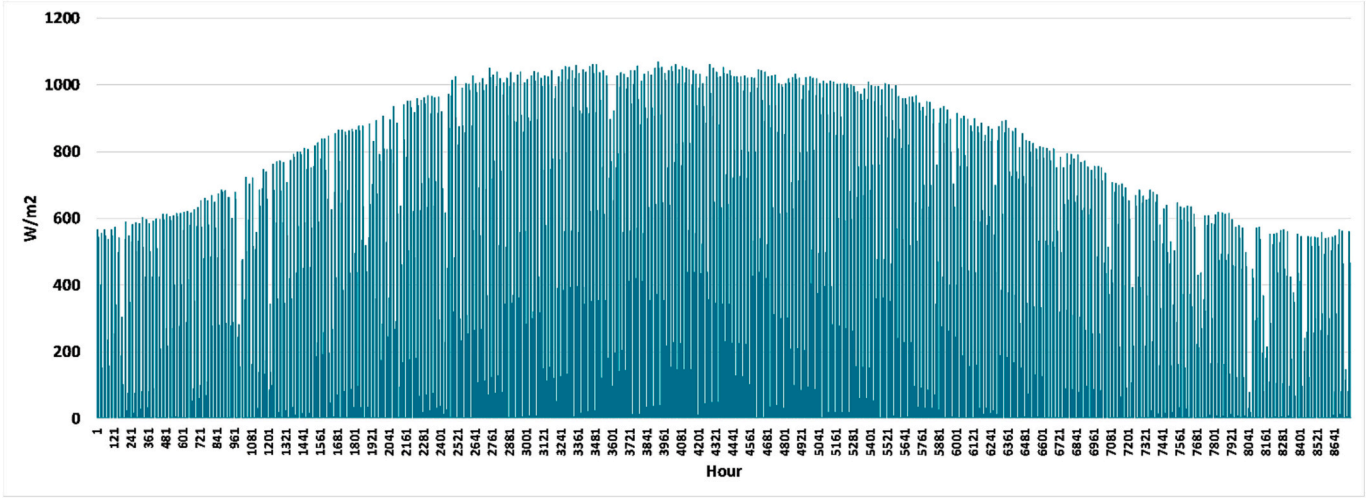

Fig. 5. The estimated hourly solar radiation of the planning site for the horizon year and one of the reduced scenarios.

Table 3
The parameters of consumers' smart devices for different types of consumers' comfort levels.

Consumer type					
1	a^{AC} = 3.45	b^{AC} = 0.06	a^{PHEV} = 0.0009	b^{PHEV} = 0.37	a^{WD} = 0.002
	b^{WD} = 0.466	a^{Light} = 0.76	b^{Light} = 0.06	a^{Ent} = 0.3	b^{Ent} = 0.03
2	a^{AC} = 3.75	b^{AC} = 0.05	a^{PHEV} = 0.00102	b^{PHEV} = 0.39	a^{WD} = 0.0025
	b^{WD} = 0.479	a^{Light} = 0.79	b^{Light} = 0.067	a^{Ent} = 0.32	b^{Ent} = 0.033
3	a^{AC} = 3.91	b^{AC} = 0.075	a^{PHEV} = 0.0011	b^{PHEV} = 0.41	a^{WD} = 0.0034
	b^{WD} = 0.502	a^{Light} = 0.81	b^{Light} = 0.072	a^{Ent} = 0.36	b^{Ent} = 0.039

Table 4
The data of simulation for the smart homes [19].

Preferred household temperature (Celsius)					
$Temp^{comf}$	23.89°	$Temp^{comf.max}$	25°	$Temp^{comf.min}$	21.11°
Household PHEV					
Capacity	12 kWh		$P^{PHEV\max}$		3.7 kWh
$E^{PHEV\max}$	10.4 kW		$E^{PHEV\min}$		9.88 kW
Household washer-dryer (1500 RPM, 8.5 kg)					
$E^{WD\max}$	5.44 kWh	$E^{WD\min}$	5.3 kWh	$P^{WD\max}$	2.2 kW
Controllable LED lights (45 W LED, 5800 lm)					
$p^{Light\ max}$	580 W	$p^{Light.comf}$	435 W		
TV (85″ QLED 8K UHD HDR Smart TV)					
TV ave. power		255 W	TV max. power		585 W
5.1-Channel home theatre system					
Ave. power		275 W	Max. power		580 W
Game console					
Ave. power		158.2 W	Max. power		310 W
Computer					
Ave. power		185 W	Max. power		295 W

deferrable, and critical loads of smart homes are calculated. Different comfort levels of consumers are considered and the values of β^{INT} and β^{DEF} are determined for each level of consumers' comfort levels.

Then, the second stage optimization process is carried out for each year of the planning horizon and 24*365 interval simulation. At the first iteration of the algorithm, the value of $\mathfrak{M}_3$ can be considered as 10 % of aggregated hourly system energy, which this value is obtained from the trial-and-error process. However, for the higher number of iterations, the exact value of $\mathfrak{M}_3$, which is calculated in the third stage problem, is replaced. At this stage, the initial values of distributed energy resource capacity, their locations, and year of installation are determined. As

Table 5
The characteristics of distributed generation units.

Electrical power output (kW)	Fuel consumption (m^3/kWh)	Operating and maintenance costs (MUs/kWh)	Investment costs (MUs) * 10^3
80	0.085	10.22	62.9632
100	0.092	11.36	70.6927
110	0.093	12.59	72.3961
120	0.097	14.35	74.3964
140	0.11	17.51	78.9321
150	0.131	18.32	86.6347
160	0.168	18.65	88.3914
180	0.189	19.02	91.2347
200	0.218	19.69	94.3921

Table 6
The input parameters of the simulation process [1].

	Parameters
Photovoltaic system	Investment cost = 1.48E+5 (MMUs/m^2.MW), Lifetime = 25 (years), Maintenance cost = 5.55E+01 (MMUs/MWh)
Wind turbine	3.5(kW) @ 250 (rpm), Cut-in speed = 3(m/s), Total length = 3 (m), Type: Up-wind horizontal rotor, noise: 37 dB(A) from 60 (m) with a wind speed 8 (m/s), Investment cost = 2.4E+03 (MMUs), Maintenance cost = 3.7E+04 (MUs/MWh)
Electrical storage system	Modules capacity = 100 (kW), Type: Lead-acid battery, Efficiency = 0.75, Investment cost = 11.285E+03 (MMUs/MWh), Operating and maintenance costs = 5.55E+02 (MMUs/MWh), Lifetime = 3500 (cycle number)
Natural gas fuel price	44 MU/kWh
PHEV	Minimum PHEVs energy = 4 kWh, Maximum PHEVs energy = 18 kWh
PHEV parking lot	Maximum number of PHEV = 500, Investment cost = 2.10E+05 (MMUs/MWh), Operating and maintenance costs = 1.0095E+04 (MMUs/MWh),
Electrical feeder	Electrical feeder fixed investment cost = 143,267 (MUs/kW), Electrical feeder length dependent investment costs = 32,641 (MUs/m)
Switching device	Investment cost = 1.13 E+5 (MUs), Lifetime = 15(years), Maintenance cost = 0.25E+01 (MUs)
Threshold for *EENSC*	5 % of aggregated hourly system energy

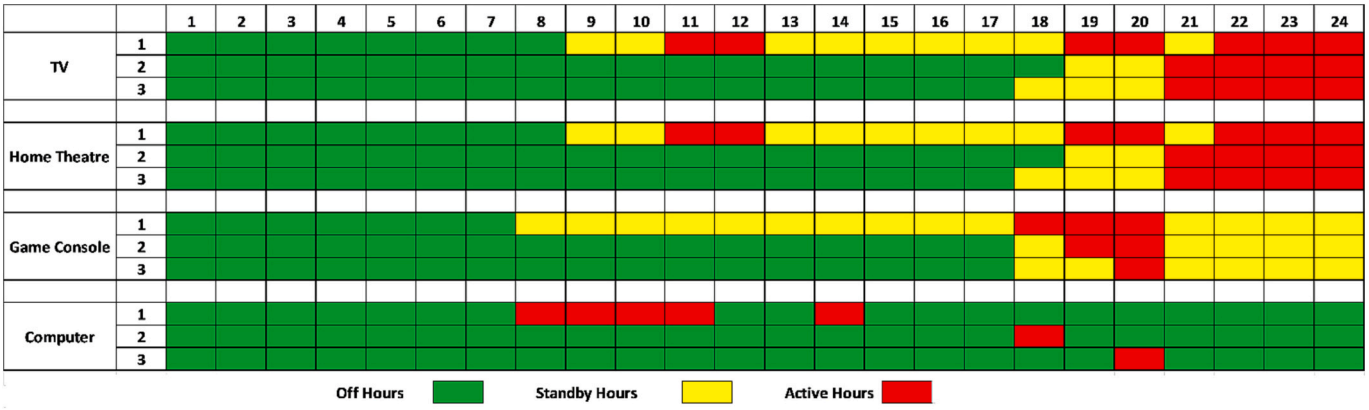

Fig. 6. The consumers' desired time of using entertainment systems for three types of consumers.

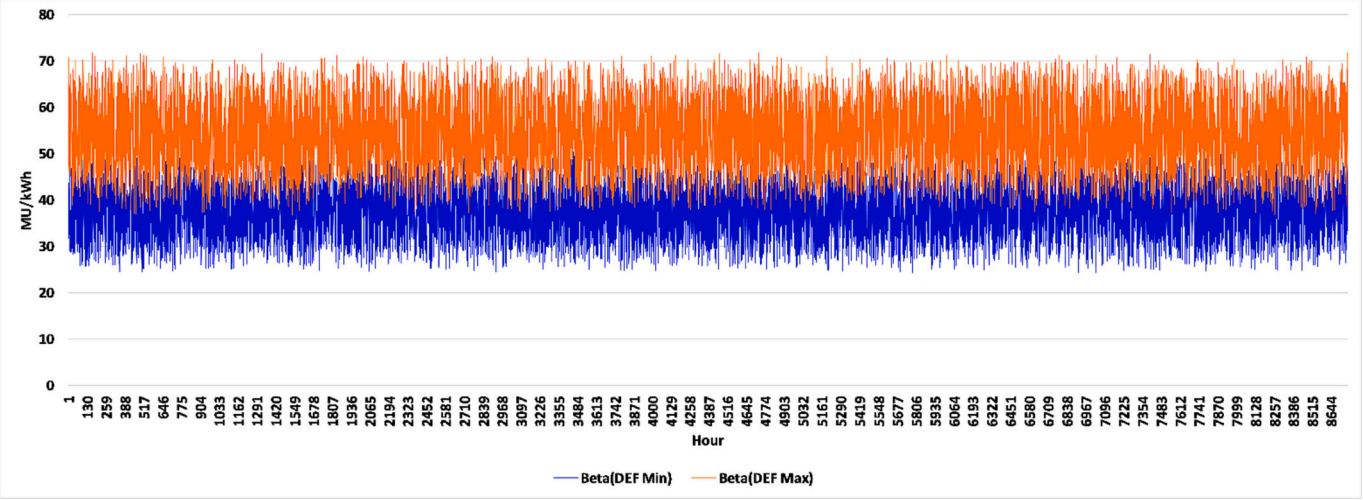

Fig. 7. The hourly minimum and maximum values of β^{DEF} for the final planning year and the three types of consumers' comfort levels.

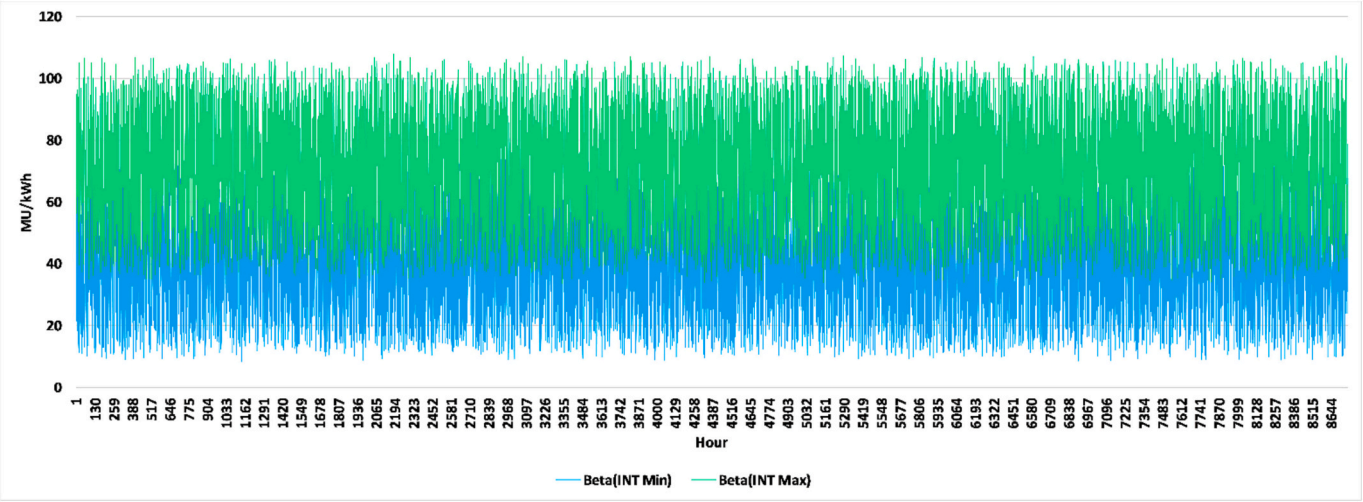

Fig. 8. The hourly minimum and maximum values of β^{INT} for the final planning year and the three types of consumers' comfort levels.

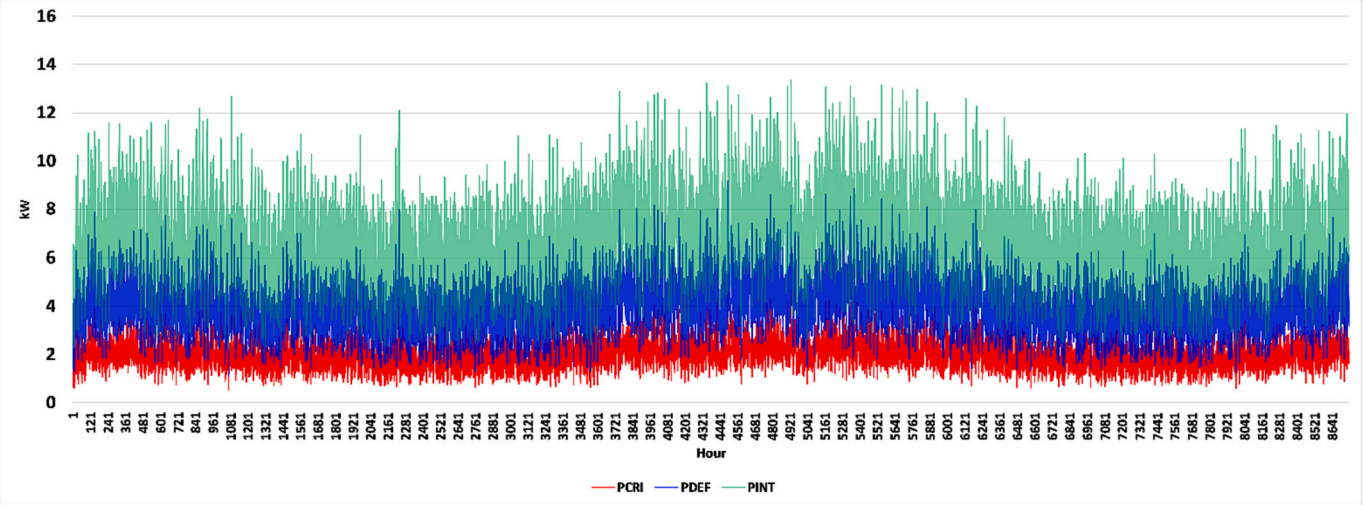

Fig. 9. The aggregated values of smart homes' critical loads, deferrable loads, and interruptible loads for the final year of the planning horizon and the three types of consumers' comfort levels.

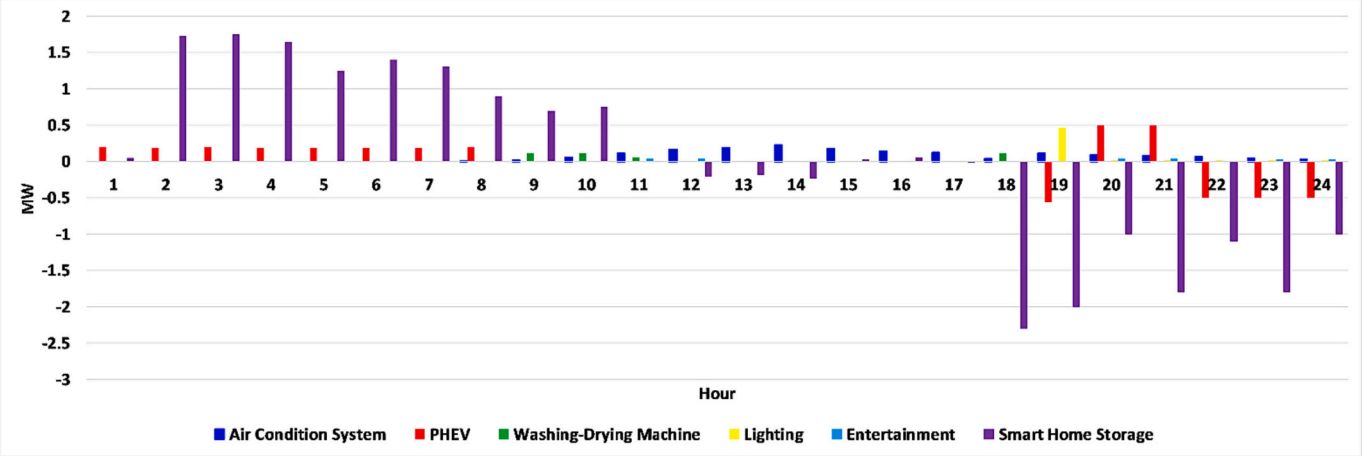

Fig. 10. The estimated values of electricity consumption of smart appliances of type 1 consumers for the final planning year and hours 2880–2903.

mentioned in the second stage optimization process, it is assumed that the installation of facilities is performed at the beginning of each year of the planning years, and the corresponding variable I_{it}^{SHEDS} is the binary decision variable of distribution facility investment for the i^{th} year of planning horizon and t^{th} hour. Thus, the computational burden of the second optimization is highly reduced based on this assumption. Hence, the third stage optimization process is performed for the worst-case interruption scenarios of smart homes in 24-hour simulation intervals. The third stage optimization process endeavors to minimize *EENSC* using the switching of the system's switches. If all of the worst-case scenarios are considered and the value of *EENSC* is less than a predefined threshold, the optimization process stops. However, if the value of *EENSC* is greater than a predefined value, the optimization process should be continued from the second stage optimization process and the distributed energy location, capacity, and time of installation should be revised. Further, the optimal values of switching devices' locations are recalculated. The output results determine the optimal values of smart home load commitment, β^{INT}, β^{DEF}, system topology, and distributed energy resource allocation and capacity.

4. Simulation results

The modified 123-bus system [2], Fig. 2, was considered for this section. The planning horizon was considered 5 years and the final year of planning was assumed 2028.

The scenario generation and reduction scenarios are presented in Table 2.

Fig. 3 presents the estimated hourly wind speed of the planning site for the horizon year and one of the reduced scenarios in Table 2. Figs. 4 and 5 depict the estimated hourly temperature and solar radiation of the planning site for the horizon year and one of the reduced scenarios in Table 2.

It was assumed that all of the test system electrical loads are residential consumers and three types of consumers were considered. Table 3 shows the parameters of consumers' smart devices for three comfort levels of consumers.

Based on the first stage optimization model, the data of smart appliances of consumers' smart homes are presented in Table 4. It is assumed that the comfort temperatures of consumers are equal and only the parameters of smart appliances are different as shown in Table 3.

Fig. 6 depicts the consumers' desired time of using entertainment systems for three types of consumers.

Table 5 presents the characteristics of distributed generation units. The lifetime of DGs is 25 years [1]. MUs and MMUs stand for monetary units and million monetary units, respectively.

Table 6 presents the input data of the simulation process.

The optimization process was performed for the first-stage problem. Fig. 7 presents the hourly minimum and maximum values of β^{DEF} for the final planning year and the three types of consumers' comfort levels. As shown in Fig. 7, the average value of the minimum and maximum values of β^{DEF} were 37.48 MU/kWh and 54.31 MU/kWh, respectively. The maximum and minimum values of β^{DEF} were 71.78 MU/kWh and 24.29 MU/kWh, respectively.

Fig. 8 depicts the hourly minimum and maximum values of β^{INT} for

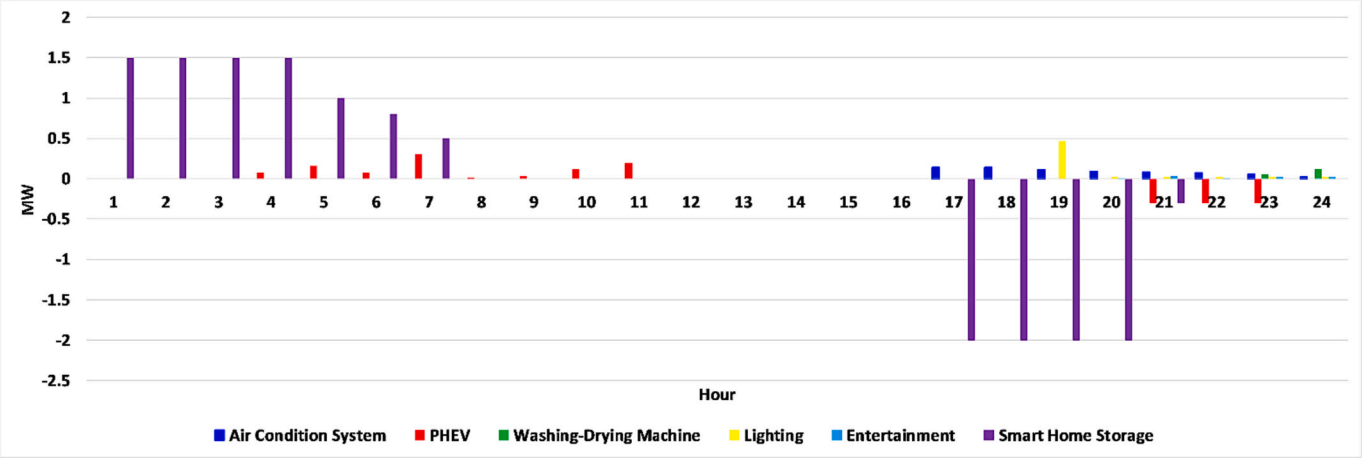

Fig. 11. The estimated values of electricity consumption of smart appliances of type 2 consumers for the final planning year and hours 2880–2903.

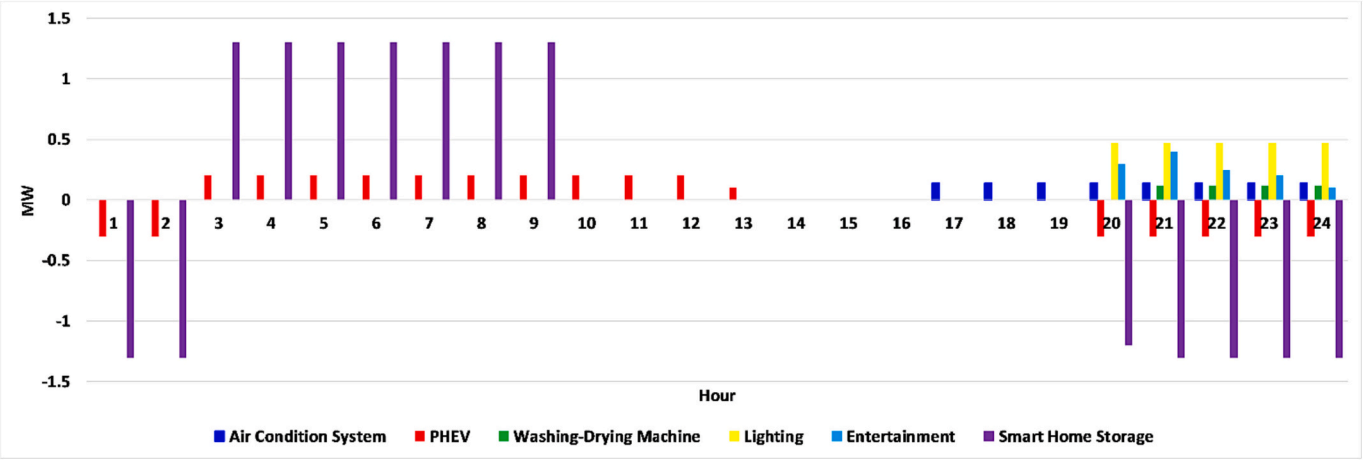

Fig. 12. The estimated values of electricity consumption of smart appliances of type 3 consumers for the final planning year and hours 2880–2903.

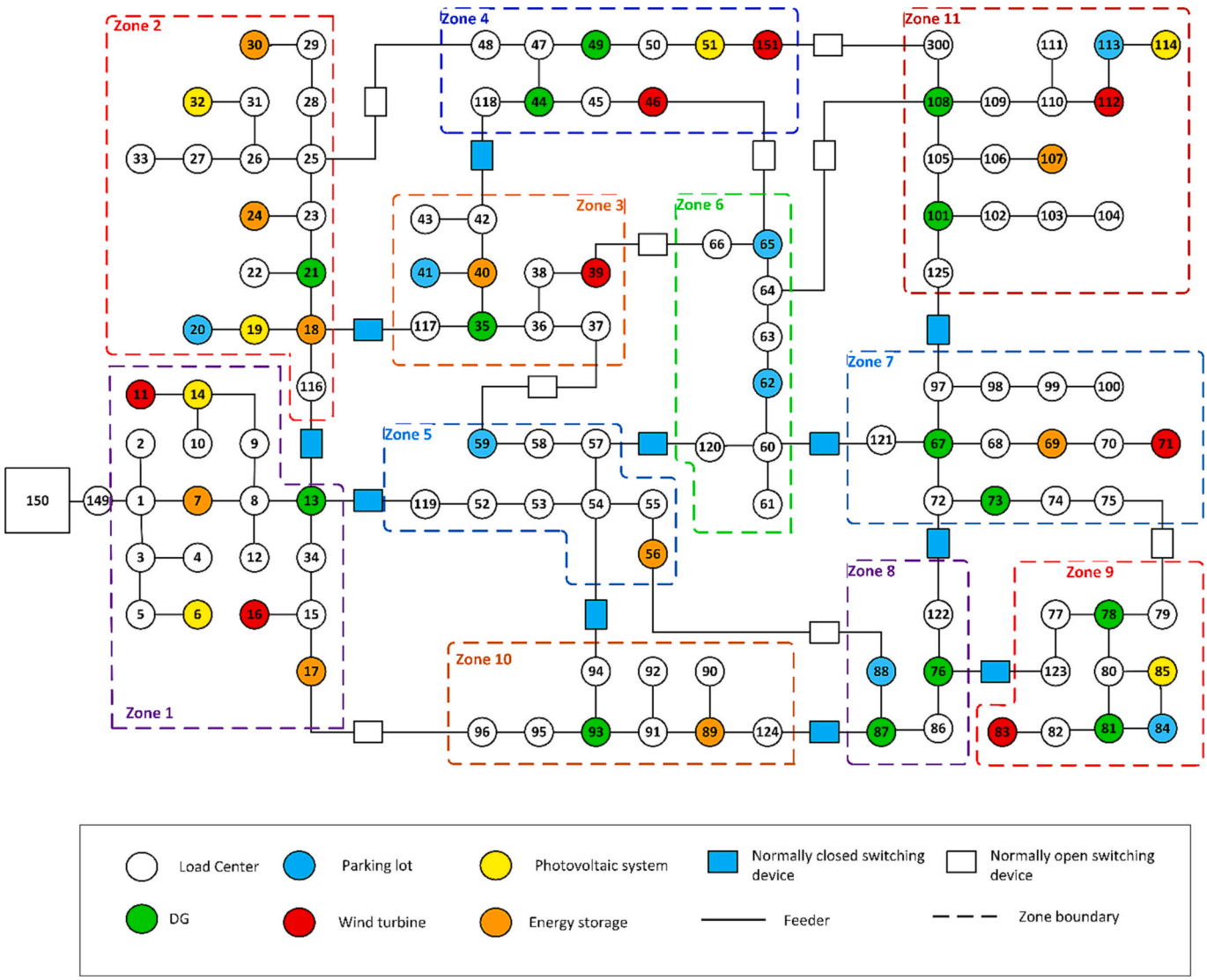

Fig. 13. The final topology of the 123-bus system for the final planning year.

Table 7
The distributed generation facilities' location and capacity.

Bus number	Capacity (kW)	Bus number	Capacity (kW)	Bus number	Capacity (kW)
13	80	21	180	35	120
44	140	48	100	49	160
67	110	73	140	76	140
78	120	81	80	87	140
93	100	101	150	108	160

the final planning year and the three types of consumers' comfort levels. As shown in Fig. 8, the average values of the minimum and maximum of β^{INT} were 41.44 MU/kWh and 70.87 MU/kWh, respectively. The maximum and minimum values of β^{INT} were 107.82 MU/kWh and 8.29 MU/kWh, respectively.

Fig. 9 presents the aggregated values of smart homes' critical loads, deferrable loads, and interruptible loads considering the values of β^{INT} and β^{DEF} for the final year of the planning horizon and one of the reduced scenarios in Table 2. The aggregated values of critical loads, deferrable loads, and interruptible loads were about 17,106.2 MWh, 17,093.55 MWh, and 22,758.31 MWh, respectively.

Based on the proposed optimization process, the optimal commitments of critical loads, deferrable loads, and interruptible loads of three types of consumers' comfort levels were performed for the 8760 h of each year of the planning horizon. Based on Eq. (16), the first stage optimization process calculated the estimated values of critical loads ($P_k^{SD\_CRI}$), deferrable loads ($P_k^{SD\_DEF}$), and interruptible loads ($P_k^{SD\_INT}$) that consist of the following smart appliances' energy consumptions:

- Critical loads ($P_k^{SD\_CRI}$) that consisted of the lighting system (at night), PHEV when its state of charge is lower than a predetermined level, and air conditioning system,
- Deferrable loads ($P_k^{SD\_DEF}$) that consisted of washing-drying machines,
- Interruptible loads ($P_k^{SD\_INT}$) that consisted of the entertainment system and PHEV when its state of charge is higher than a predetermined level.

Fig. 10 depicts the estimated values of electricity consumption of smart appliances of type 1 consumers for the final planning year and hours 2880–2903. As shown in Fig. 10, the aggregated values of the air-conditioning system, PHEVs, washing-drying machine, lighting, and entertainment systems were about 1.71 MWh, 0.49 MWh, 0.41 MWh, 0.586 MWh, and 0.259 MWh, respectively.

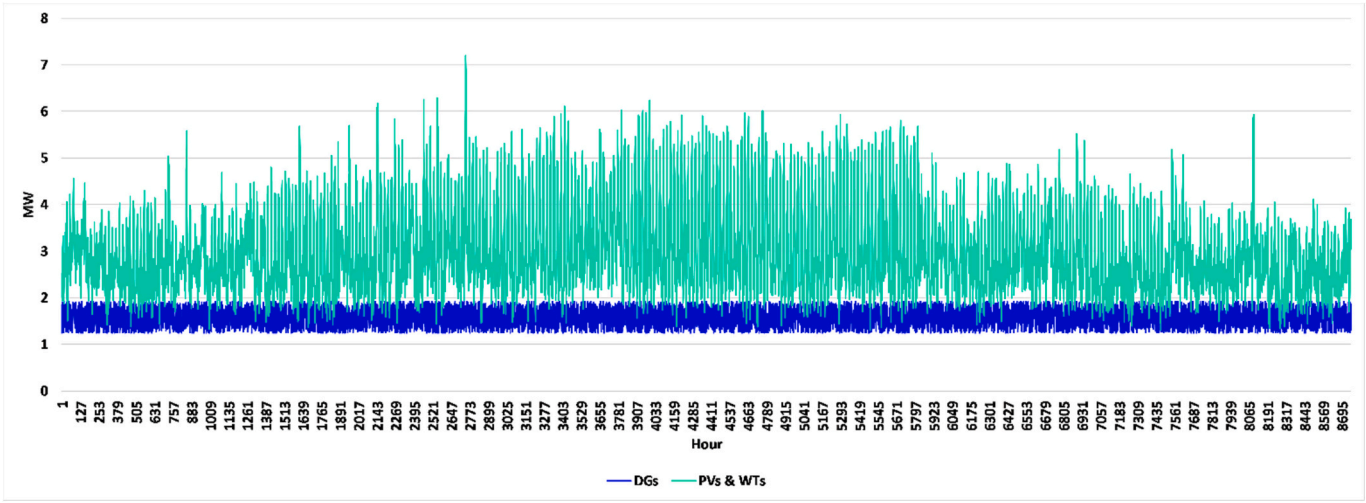

Fig. 14. The estimated values of hourly electricity generation of wind turbines, photovoltaic arrays, and distributed generation facilities for the final year of the planning horizon and one of the reduced scenarios.

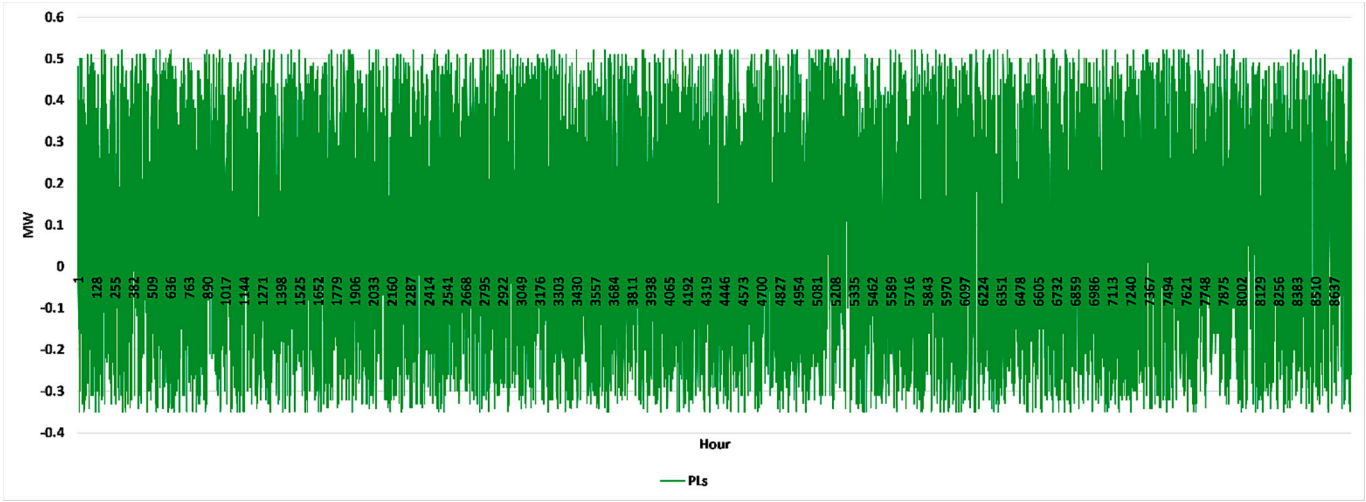

Fig. 15. The estimated values of hourly electricity transactions of parking lots for the final year of the planning horizon and one of the reduced scenarios.

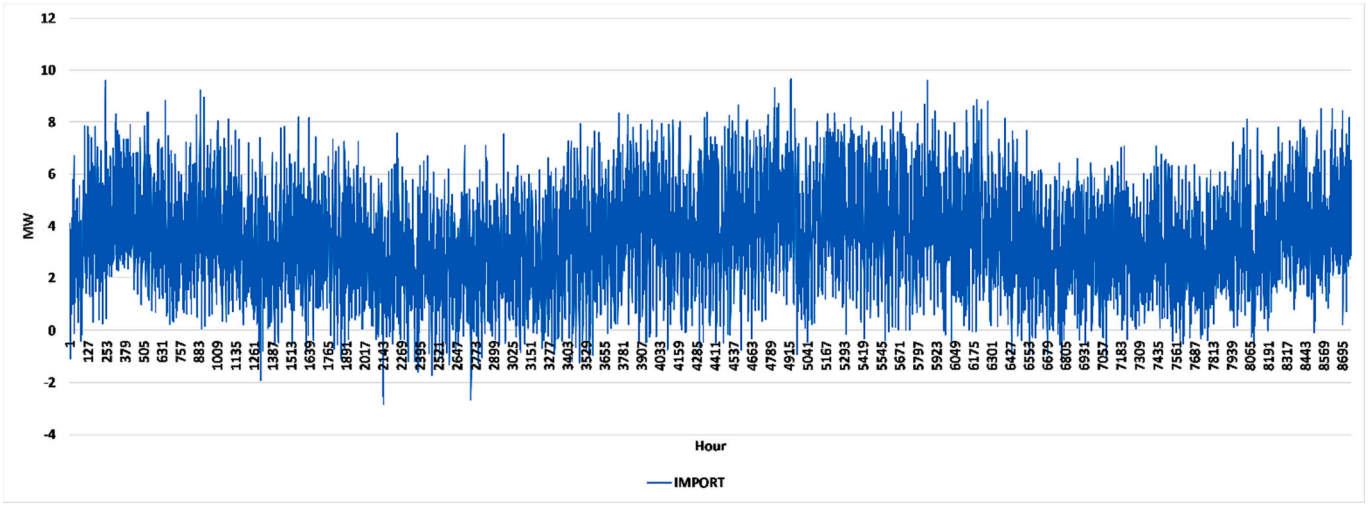

Fig. 16. The estimated values of hourly electricity transactions of the distribution system with the wholesale market for the final year of the planning horizon and one of the reduced scenarios.

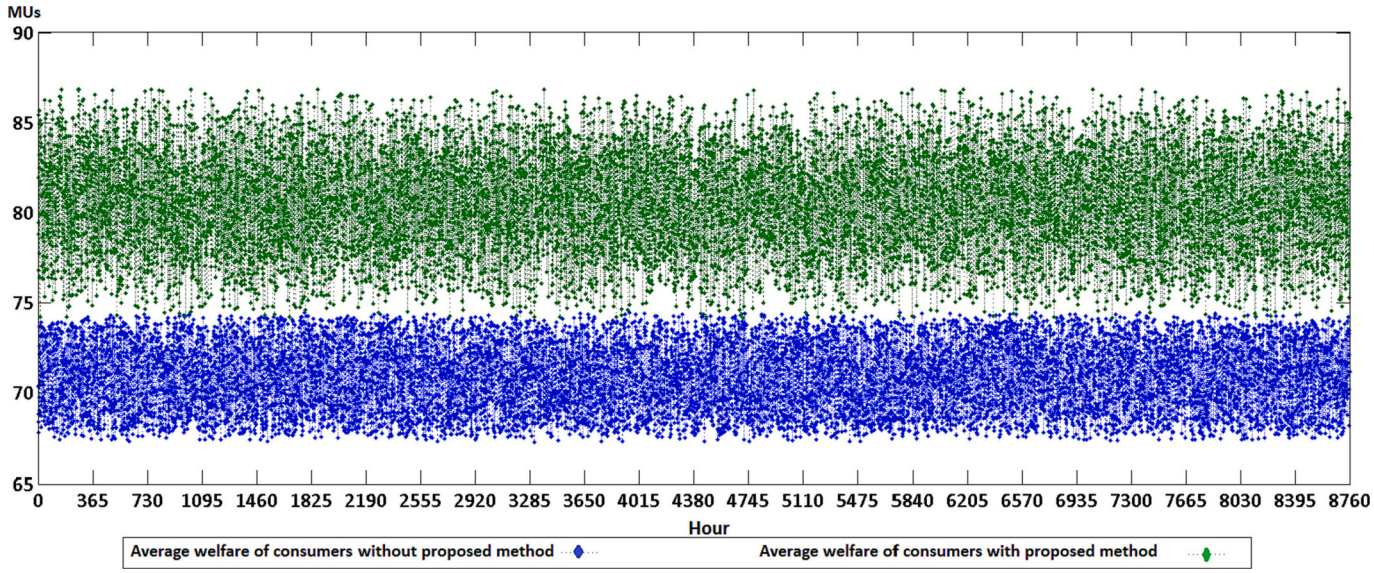

Fig. 17. The average values of type 1 consumers' welfare for the first and second cases for the final year of the planning horizon.

Fig. 11 shows the estimated values of electricity consumption of smart appliances of type 2 consumers for the final planning year and hours 2880–2903. As shown in Fig. 11, the aggregated values of the air-conditioning system, PHEVs, washing-drying machine, lighting, and entertainment systems were about 0.72 MWh, 0.082 MWh, 0.293 MWh, 0.61 MWh, and 0.133 MWh, respectively.

Fig. 12 presents the estimated values of electricity consumption of smart appliances of type 3 consumers for the final planning year and hours 2880–2903. As shown in Fig. 12, the aggregated values of the air-conditioning system, PHEVs, washing-drying machine, lighting, and entertainment systems were about 1.12 MWh, 0 MWh, 0.48 MWh, 2.368 MWh, and 1.25 MWh, respectively.

Then, the second-stage optimization process was performed. Fig. 13 shows the final topology of the 123-bus system for the final planning year. The optimization process determined the location and capacity of distributed energy resources and system topology. The system consisted of eleven microgrids.

Table 7 presents the location and capacity of distributed energy resources for the final year of the planning horizon.

Fig. 14 depicts the estimated values of hourly electricity generation of wind turbines, photovoltaic arrays, and distributed generation facilities for the final year of the planning horizon and one of the reduced scenarios in Table 2. The aggregated value of Wind Turbines (WTs) and PhotoVoltaic (PV) array electricity generation was about 12,309.14 MWh for the final year. Further, the aggregated value of electricity generation of distributed generation facilities was about 13,887.49 MWh for the final year of the planning horizon.

Fig. 15 shows the estimated values of hourly electricity transactions of parking lots for the final year of the planning horizon and one of the reduced scenarios in Table 2. The aggregated value of electricity transactions of parking lots was about 729.43 MWh for the final year. Fig. 16 shows the estimated values of hourly electricity transactions of the distribution system with the wholesale market for the final year of the planning horizon and one of the reduced scenarios in Table 2. The aggregated value of electricity transactions of the distribution system was about 30,032.1 MWh for the final year.

The following two cases were considered in the optimization process:

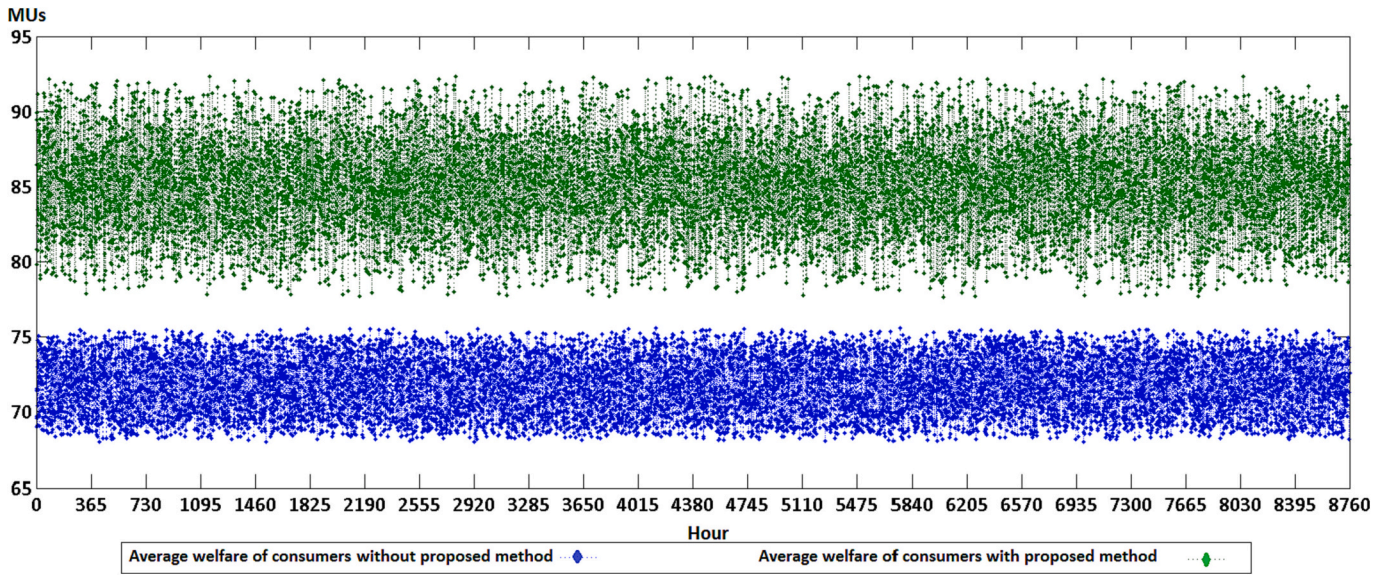

Fig. 18. The average values of type 2 consumers' welfare for the first and second cases for the final year of the planning horizon.

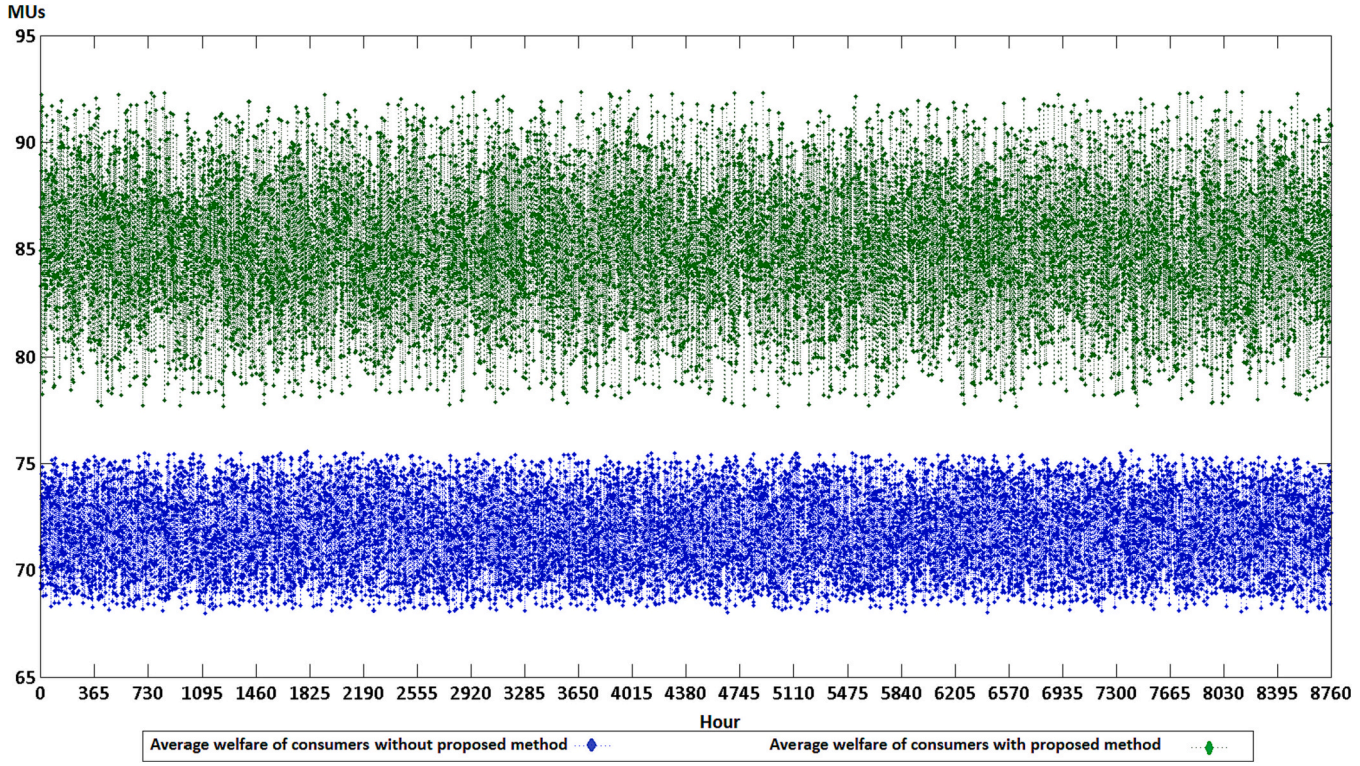

Fig. 19. The average values of type 3 consumers' welfare for the first and second cases for the final year of the planning horizon.

1. The first case did not consider the first-stage optimization process and only performed the *sec*ond and third stages of the proposed model.
2. The second case performed the proposed model.

The simulation was carried out for the first and second cases considering the worst-case external shock for each hour of the planning horizon. The values of the consumers' welfare for the worst-case external shock were calculated for the first and second cases.

Fig. 17 shows the average values of type 1 consumers' welfare for the first and second cases for the final year of the planning horizon. As shown in Fig. 17, the average values of consumers' welfare were 70.88 MUs and 80.56 MUs for the first and second cases, respectively. The proposed model increased the consumers' welfare by about 13.65 % for the worst-case external shocks.

Fig. 18 presents the average values of type 2 consumers' welfare for the first and second cases for the final year of the planning horizon. As shown in Fig. 18, the average values of consumers' welfare were 71.77 MUs and 85.08 MUs for the first and second cases, respectively. The proposed model increased the consumers' welfare by about 18.54 % for

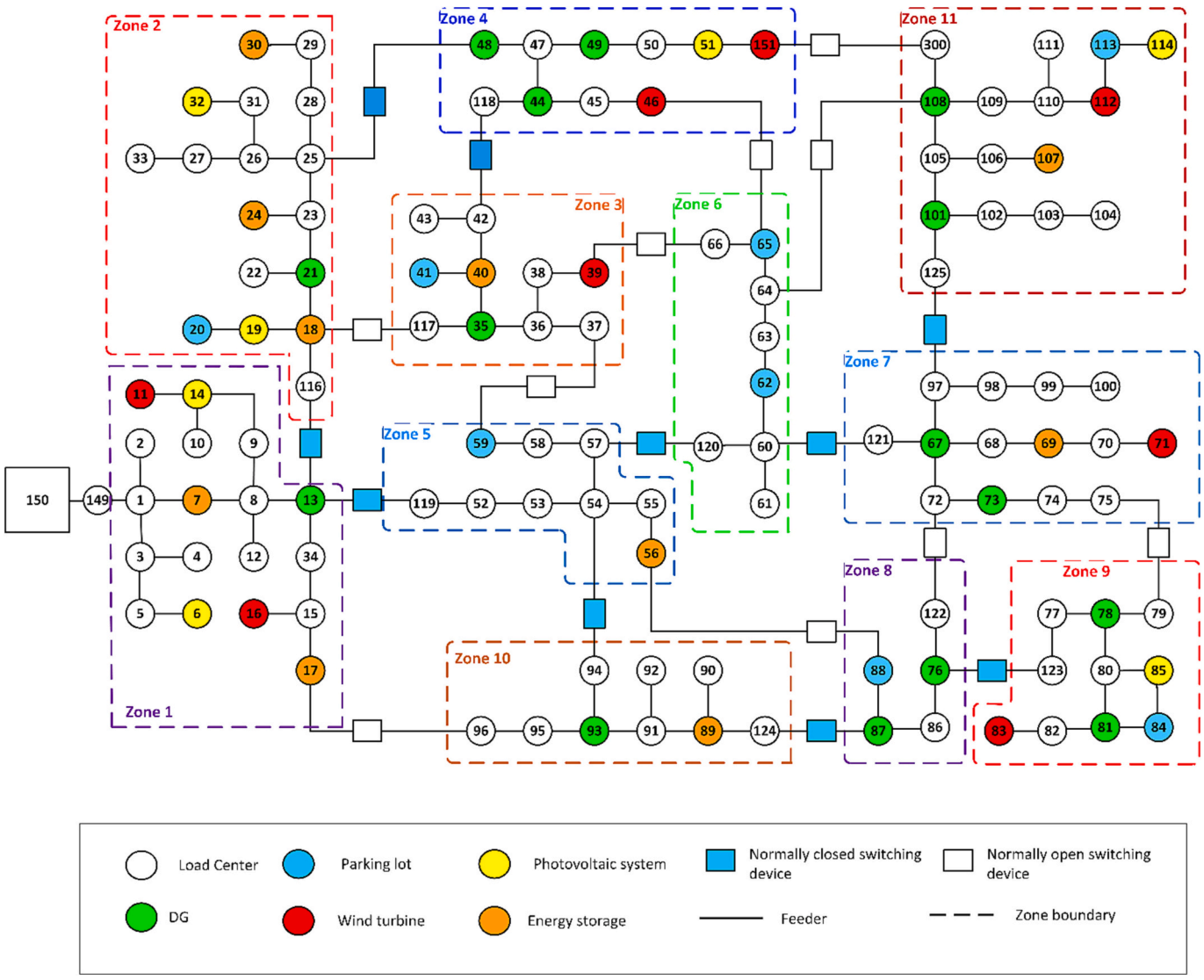

Fig. 20. The optimal topology of the system considering the worst-case external shock that occurred in lines #18–117 and #72–122.

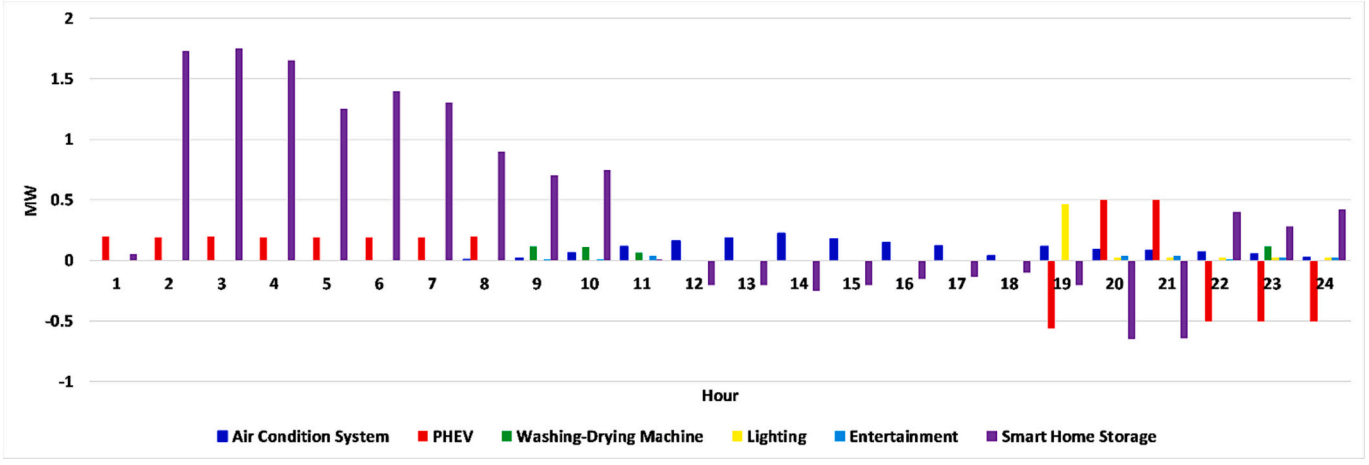

Fig. 21. The estimated values of electricity consumption of smart appliances of type 1 consumers for the external shock.

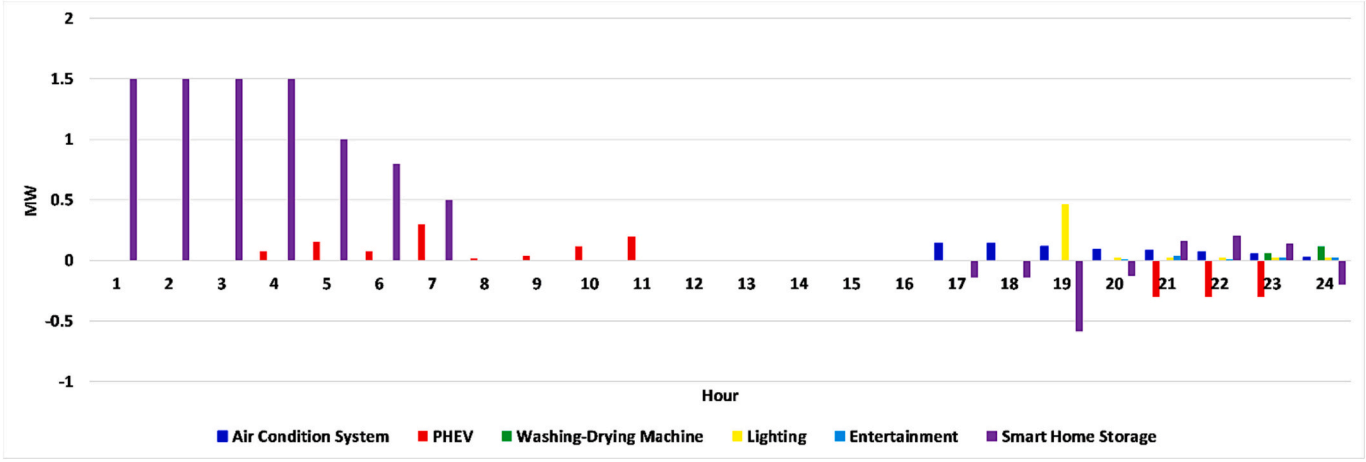

Fig. 22. The estimated values of electricity consumption of smart appliances of type 2 consumers for the external shock.

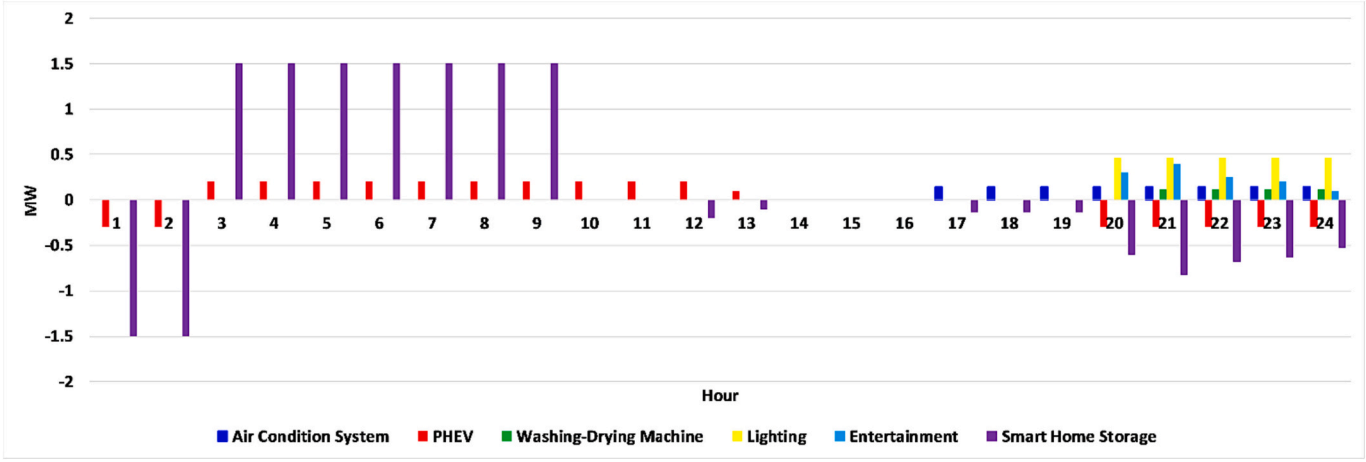

Fig. 23. The estimated values of electricity consumption of smart appliances of type 3 consumers for the considered external shock.

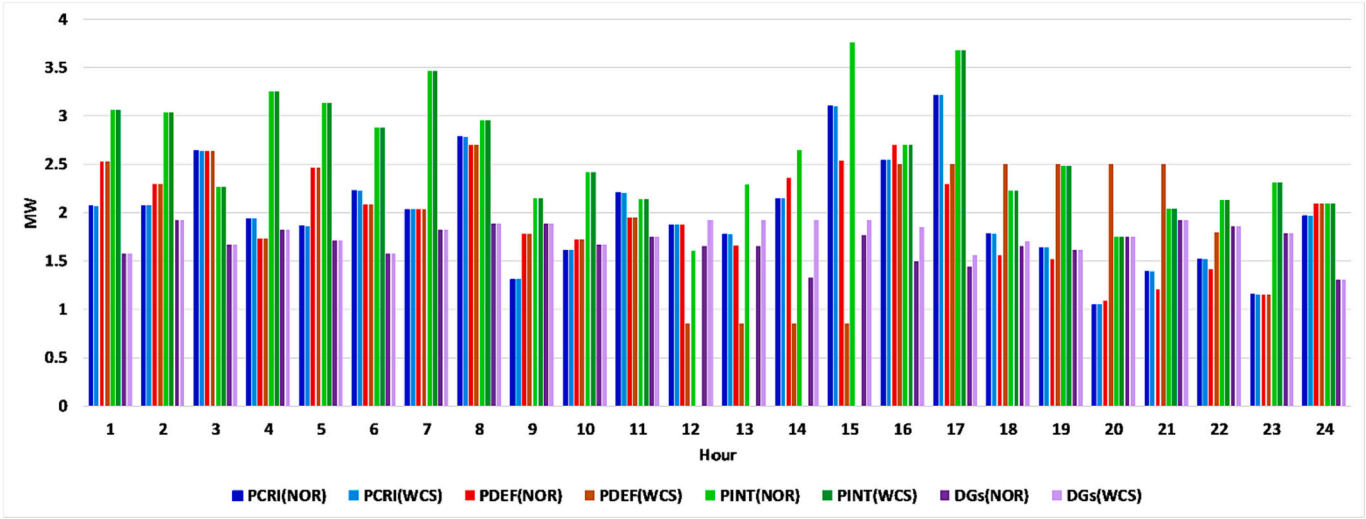

Fig. 24. The estimated values of electricity consumption of smart homes and electricity generation of distributed energy resources for normal and the worst-case external shock conditions.

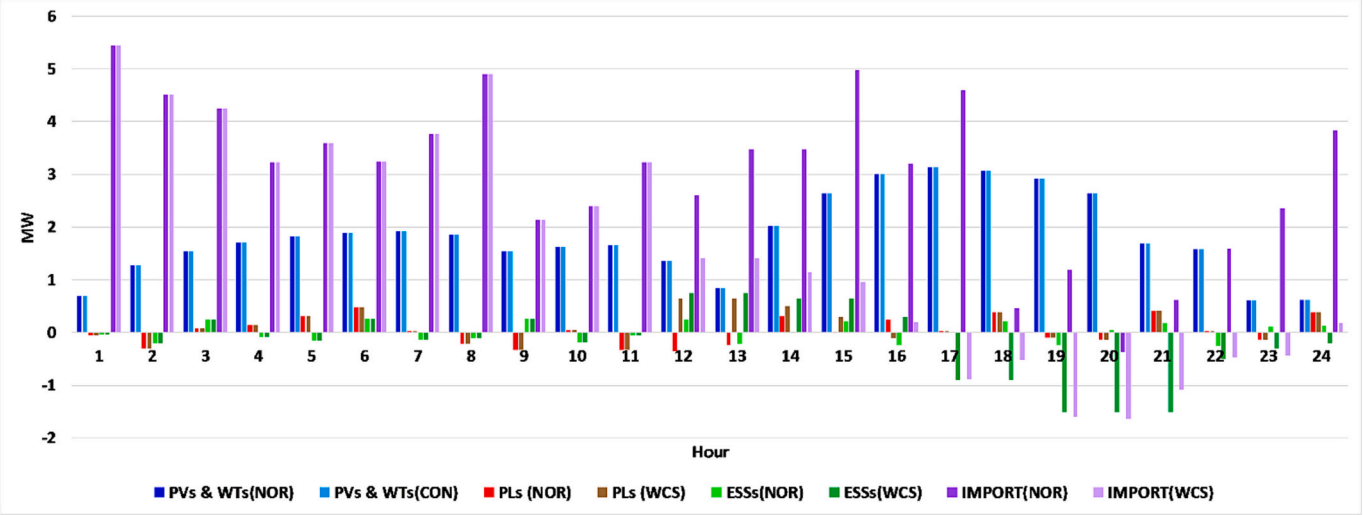

Fig. 25. The estimated values of electricity generation of intermittent energy resources, parking lots' and energy storages' electricity transactions, and distribution system transactions with the wholesale market for normal and the worst-case external shock conditions.

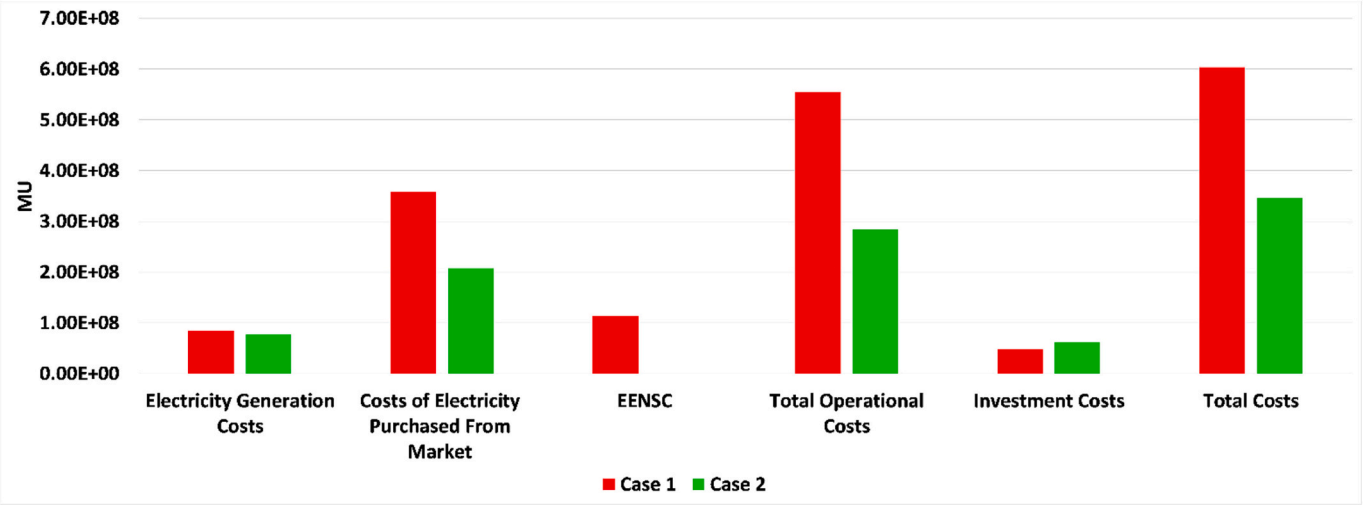

Fig. 26. The electricity generation costs, energy purchased costs, *EENSC*, and investment costs for the first and second cases.

Table 8
The characteristics of the simulation in the first and second case studies.

Case study number	Number of iterations	Stage of optimization	CPU time (sec) for the final iteration	Cont. variables for the final iteration	Disc. variables for the final iteration
1	–	–	–	–	–
	1	Stage 2	12,328	275,981	221,981
	1	Stage 3	1202	1,254,202	602,962
2	2	Stage 1	891	389,257	324,174
	2	Stage 2	23,259	536,989	431,928
	2	Stage 3	1407	1,298,369	617,874

the worst-case external shocks. Fig. 19 shows the average values of type 3 consumers' welfare for the first and second cases for the final year of the planning horizon.

As shown in Fig. 19, the average values of consumers' welfare were 71.78 MUs and 85.67 MUs for the 1st and 2nd cases, respectively. The proposed model increased the consumer's welfare by about 19.35 % for the worst-case external shocks.

One of the worst-case external shocks was the simultaneous outage of lines 18–117 and 72–122 that occurred in the 2892nd hour and corresponded to 12:00 AM of day 5/1/2027. Fig. 20 presents the third-stage optimization simulation results for this worst-case external shock.

Fig. 21 depicts the estimated values of electricity consumption of smart appliances of type 1 consumers for the considered worst-case external shock.

As shown in Fig. 21, the aggregated values of the air-conditioning system, PHEVs, washing-drying machine, lighting, and entertainment systems were about 1.71 MWh, 0.49 MWh, 0.41 MWh, 0.586 MWh, and 0.19 MWh, respectively. By comparing Fig. 21 and Fig. 10, it can be concluded that only the entertainment loads were reduced by about 0.069 MWh, and all of the critical loads of type 1 consumers were supplied using the proposed method.

Fig. 22 shows the estimated values of electricity consumption of smart appliances of type 2 consumers for the considered worst-case external shock. As shown in Fig. 22, the aggregated values of the air-conditioning system, PHEVs, washing-drying machine, lighting, and entertainment systems were about 0.72 MWh, 0.082 MWh, 0.175 MWh, 0.586 MWh, and 0.104 MWh, respectively. By comparing Fig. 22 and Fig. 11, it can be concluded that all of the critical loads of type 2

consumers were supplied using the proposed method.

Fig. 23 presents the estimated values of electricity consumption of smart appliances of type 3 consumers for the considered worst-case external shock. As shown in Fig. 23, the aggregated values of the air-conditioning system, PHEVs, washing-drying machine, lighting, and entertainment systems were about 1.12 MWh, 0 MWh, 0.48 MWh, 2.345 MWh, and 1.25 MWh, respectively.

By comparing Fig. 23 and Fig. 12, it can be concluded that all of the critical loads of type 3 consumers were supplied using the proposed method.

Fig. 24 presents the estimated values of electricity consumption of smart homes and electricity generation of distributed energy resources for normal and worst-case external shock conditions. As shown in Fig. 24, it can be concluded that the critical loads were fully supplied in the worst-case external shock. Further, the deferrable loads were reduced from 1.8726 MWh to 0.85 MWh, the interruptible loads were reduced from 1.6051 MWh to 0.85 MWh, and finally, the distributed generation electricity generation was increased from 1.65 MWh to 1.92 MWh.

Fig. 25 presents the estimated values of electricity generation of intermittent energy resources, parking lots, and energy storages' electricity transactions, distribution system transactions with the wholesale market for normal and the worst-case external shock conditions. As shown in Fig. 25, it can be concluded that the parking lots' electricity transactions increased from −0.35 MWh to 0.65 MWh, and electrical energy storages increased the electricity injection from 0.238 MWh to 0.75 MWh. The distribution system reduced imported energy from the wholesale market from 2.6 MWH to 1.4 MWh based on the fact that the external shock changed the topology of the system and the optimal load flow of the third stage problem endeavored to find the optimal topology and energy resources dispatch considering the double fault condition of the system.

Fig. 26 shows the electricity generation costs, energy purchased costs, *EENSC*, and investment costs for the first and second cases. By comparing the total costs of the first case and second case, it can be concluded that the proposed method reduced the total costs of the system by about 42.62 % considering the consumers' optimal load commitment. Further, the *EENSC* of the system was reduced from 113 million MUs to 0.284 million MUs based on the fact that all of the critical loads of consumers were supplied, and the deferrable and interruptible loads were scheduled by the consumers to gain more profit.

The characteristics of the simulation in the first and second case studies are presented in Table 8. The number of iterative processes is based on Fig. 1. The simulation was carried out on a PC (Intel Core i7–13,700 processor, 128 GB memory, DDR4 3200 MT).

5. Conclusion

This paper explored the effectiveness of a tri-stage optimization process for expansion planning of a self-healing distribution system. The consumer comfort levels were considered in the model and the smart appliances' commitments were modeled. The first stage problem modeled the smart homes' appliances consisted of washing-drying machines, air conditioning systems, plug-in hybrid electric vehicles, lighting systems, and entertainment systems. The optimal scheduling of smart appliances was determined considering the worst-case external shocks. Then, in the second stage, the optimal expansion planning of the system was carried out considering the first stage objective function. Finally, in the third stage problem, the optimal topology and distributed energy resources dispatch were determined considering the worst-case external shocks of the first stage problem. The 123-bus system was utilized to assess the model. Two cases were considered in the simulation process. The first case did not encounter the consumer comfort levels in the expansion planning practice. The second case utilized the proposed model. The investment costs of the second case expanded by about 28.95 % regarding the first case. However, the aggregated operational costs of the second case were reduced by about 48.88 % regarding the base case. The proposed model decreased the aggregated investment and operational costs of the system by about 42.62 % regarding the first case result. In conclusion, the proposed model decreased significantly the system-aggregated costs and endeavored to maximize consumer comfort levels. The authors are working on the modeling of other smart appliances and defining a new framework for the optimization process to reduce the computational burden.

CRediT authorship contribution statement

Hossein Hosseini: Writing – original draft, Investigation, Data curation. **Mehrdad Setayesh Naza:** Supervision, Methodology, Conceptualization. **Miadreza Shafie-khah:** Validation, Formal analysis. **João P.S. Catalão:** Writing – review & editing, Visualization.

Declaration of competing interest

The authors declare that they have no known competing financial interests or personal relationships that could have appeared to influence the work reported in this paper.

Data availability

Data will be made available on request.

References

[1] M. Setayesh Nazar, P. Jafarpour, M.R. Shafie-khah, J.P.S. Catalão, Optimal planning of self-healing multi-carriers energy systems considering integration of smart buildings and parking lots energy resources, Energy 286 (2024) 128674.
[2] M. Aboutalebi, M. Setayesh Nazar, M. Shafie-khah, J.P.S. Catalão, Optimal scheduling of self-healing distribution systems considering distributed energy resource capacity withholding strategies, Int. J. Electr. Power Energy Syst. 136 (2022) 107662.
[3] Y. Gilasi, S.H. Hosseini, H. Ranjbar, Resiliency-oriented optimal siting and sizing of distributed energy resources in distribution systems, Electr. Pow. Syst. Res. 208 (2022) 107875.
[4] T. Akbari, S. Zolfaghari Moghaddam, A scenario-based robust distribution expansion planning under ellipsoidal uncertainty set using second-order cone programming, Electr. Pow. Syst. Res. 213 (2022) 108773.
[5] S. Zhou, Y. Han, P. Yang, K. Mahmoud, M. Lehtonen, M.M.F. Darwish, A.S. Zalhaf, An optimal network constraint-based joint expansion planning model for modern distribution networks with multi-types intermittent RERs, Renew. Energy 194 (2022) 137–151.
[6] M.G. Firoozjaee, M.K. Sheikh-El-Eslami, A hybrid resilient static power system expansion planning framework, Int. J. Electr. Power Energy Syst. 133 (2021) 107234.
[7] S.M. Masoumi-Amiri, M. Shahabi, T. Barforoushi, Interactive framework development for microgrid expansion strategy and distribution network expansion planning, Sustainable Energy, Grids and Networks 27 (2021) 100512.
[8] A. Nasri, A. Abdollahi, M. Rashidinejad, Multi-stage and resilience-based distribution network expansion planning against hurricanes based on vulnerability and resiliency metrics, Int. J. Electr. Power Energy Syst. 136 (2022) 107640.
[9] A. Shahbazi, J. Aghaei, S. Pirouzi, M. Shafie-khah, J.P.S. Catalao, Hybrid stochastic/robust optimization model for resilient architecture of distribution networks against extreme weather conditions, Int. J. Electr. Power Energy Syst. 126 (2021) 106576.
[10] S. Mousavizadeh, T. Ghanizadeh Bolandi, M.R. Haghifam, Resiliency analysis of electric distribution networks: a new approach based, Int. J. Electr. Power Energy Syst. 117 (2020) 105669.
[11] D. Wu, X. Ma, S. Huang, T. Fu, P. Balducci, Stochastic optimal sizing of distributed energy resources for a cost effective and resilient microgrid, Energy 198 (2020) 117284.
[12] M.A. Gilani, A. Kazemi, M. Ghasemi, Distribution system resilience enhancement by microgrid formation considering distributed energy resources, Energy 191 (2020) 116442.
[13] M. Bessani, J. Massignan, R. Fanucchi, M. Camillo, J. London, A. Delbem, C. Maciel, Probabilistic assessment of power distribution systems resilience under extreme weather, IEEE Sys. Journal 13 (2) (2019) 1747–1756.
[14] W. Yuan, J. Wang, F. Qiu, C. Chen, C. Kang, B. Zeng, Robust optimization-based resilient distribution network planning against natural disasters, IEEE Trans. Smart Grid 7 (2016) 2817–2826.
[15] M. Zare-Bahramabadi, A. Abbaspour, M. Fotuhi-Firuzabad, M. Moeini-Aghtaie, Resilience-based framework for switch placement problem in power distribution systems, IET Gener. Transm. Distrib. 12 (5) (2018) 1223–1230.

[16] S. Mishra, C. Bordin, A. Tomasgard, A. Palua, A multi-agent system approach for optimal microgrid expansion planning, Int. J. Electr. Power Energy Syst. 109 (2019) 696–709.
[17] Y. Lin, Z. Bie, Tri-stage optimal hardening plan for a resilient distribution system considering reconfiguration and DG islanding, Appl. Energy 210 (2018) 1266–1279.
[18] H. Zakernezhad, M. Setayesh Nazar, M.R. Shafie-khah, J.P.S. Catalão, Multi-level optimization framework for resilient distribution system expansion planning with distributed energy resources, Energy 214 (2021) 118807.
[19] M. Tehrani Nowbandegani, M. Setayesh Nazar, M. Shafie-khah, J.P.S. Catalão, Demand response program integrated with electrical energy storage systems for residential consumers, IEEE Sys. Journal 16 (3) (2022) 4313–4324.
[20] A. Kavousi-Fard, A. Zare, A. Khodaei, Effective dynamic scheduling of reconfigurable microgrids, IEEE Trans. on Power Syst. 33 (5) (2018) 5519–5530.